University of Stuttgart
Institute for Modelling Hydraulic and Environmental Systems
Department of Stochastic Simulation and Safety Research for Hydrosystems

Yomer Cisneros

Optimization of irrigation operations: A case study of irrigation management in Punjab-Pakistan

Master's Thesis

Optimization of irrigation operations: A case study of irrigation management in Punjab-Pakistan

Submitted by

Yomer Cisneros

Matriculation Number: 3439717

Examiner: Prof. Dr.-Ing. Habil. Sergey Oladyshkin

Supervisor: M.Sc. Fahad Ejaz

Institute for Modeling Hydraulic and Environmental Systems
Department of Stochastic Simulation and Safety Research for Hydrosystems

Stuttgart, 1^{st} November 2021

Acknowledgements

I am extraordinarily grateful to my esteemed advisor M.Sc. Fahad Ejaz, for his wise guidance, critical and innovative insights, and very strong commitment towards this study.

I would like to extend my sincere thanks to my supervisor Professor Dr.-Ing. Sergey Oladyshkin for his support and advice, which contributed to the success of this study.

Author declaration

I declare that I have developed and written the enclosed thesis completely by myself and that I have not used sources or means without declaration in the text. Any thoughts from others or literal quotations are clearly marked.

The thesis was not used in the same or in a similar version to achieve an academic grading or is being published elsewhere.

The enclosed electronic version is identical to the printed versions.

Date	Signature

Contents

List of Figures

List of Tables

Abbreviations and symbols

Table 1.: Abbreviations and symbols

Abbreviation	**Description**
IBIS	Indus Basin Irrigation System
R^2	Coefficient of determination
NSE	Nash-Sutcliffe Efficiency
KGE	Kling-Gupta Efficiency
PBIAS	Percent bias
PID	Punjab Irrigation Department
PDF	Probability Density Function
MSE	Mean Square Error
IRSA	Indus River System Authority
PMIU	Project Monitoring and Implementation Unit
IWT	Indus Water Treaty
MLE	Maximum Likelihood Estimate
WEAP	Water Evaluation And Planning System
IWRM	Integrated Water Resources Management

Abstract

Water resource is being stressed due to increasing levels of social demands, particularly in emerging and least developed nations. The arid and agro-based country of Pakistan is highly dependent on Indus Basin Irrigation System (IBIS), one of the biggest contiguous irrigation networks in the world, mainly fed by the Indus River, and its Eastern tributaries Jhelum, Chenab, Ravi, and Sutlej. With limited water resources, irrigated agriculture needs to improve its efficiency and equitable distribution. This study aims to develop a flexible network model that involves a series of nodes interconnected via links to characterize the Punjab irrigation within the IBIS system. The model is calibrated by using Bayesian Monte Carlo method, where available knowledge about gain/loss parameters is updated with the information in observed data.

After a rigorous calibration and validation, the model performance was assessed through the use of the coefficient of determination (R^2), Nash–Sutcliffe Efficiency (NSE), Kling-Gupta Efficiency (KGE), and Percent bias (PBIAS). The overall results of the proposed network model were acceptable for both calibration and validation periods, except in some particular barrage tails. Nevertheless, due to the complexity of the irrigation network and the simultaneous calibration for the entire system, the model behavior is considered satisfactory. The optimized routing gain/loss coefficients coherently explained the field conditions in the study area.

The findings in this study imply that zones with higher flow discharges are prone to large uncertainties. In addition, posterior probability distributions of gain/loss coefficients suggest an adequate identification of the parameter uncertainties, with changes in the prior probability distributions. It also demonstrates how a selection of prior distribution bounds and model parameters could improve the reliability and robustness of the model.

The model would be helpful to water resource managers involved in agricultural water management in Punjab province. However, the utility of the model should be taken with great care because there are still uncertainties in the modeling results due to the conceptual nature and the quality of input data.

Keywords: Irrigation system, flexible network model, Bayesian Monte Carlo, calibration, uncertainty quantification.

1. Introduction

1.1. Problem Statement

Pakistan´s economy is highly dependent on agriculture. This sector relies mostly on surface irrigation systems, withdrawing more than 78% of the available water only for this purpose because of the aridity of its lands [1]. Pakistan has a complex water landscape; the irrigation system depends mainly on the Indus Basin, which is continuously riddled with human interventions, such as the Indus Basin Irrigation System (IBIS). With a total area of 0.52 million km^2 of Pakistan´s territory, Indus Basin covers a big part of Punjab province and its irrigation network. The IBIS is one of the biggest contiguous irrigation systems around the planet, encompassing rivers, dense network links and canals. This system is mainly fed by the Indus River and its two Eastern Jhelum-Chenab tributaries. The irrigation network is responsible to irrigate about 8.4 million hectares of the cultivable area through 58,000 outlets. The operation and maintenance of the system are the prime responsibility of the Punjab Irrigation Department (PID). Regardless of such a large irrigation system and its significance in the country's economy, water security is undermined by inequitable irrigation distribution service and hydraulic inefficiency that contributes to low water productivity in agriculture [1].

The management of the complex Punjab Irrigation System is itself a big challenge. Punjab water supply operation has been based on a heuristic approach, which depends mainly on expert judgment and does not necessarily offer an adequate response to changes of real-time conditions and short periods. Thus, the overall irrigation efficiency of Punjab is only 40% [1], being a matter of concern for decision-makers.

Although the huge efforts for optimizing the surface water, it has not been enough to ensure a stable distribution throughout the Punjab areas. Thus, there is a need to characterize the entire Punjab network system through water distribution model capable of handling the system constraints due to links and canal demands. Therefore, this will help to the authorities to make more informed decisions about the water distribution.

The proposed distribution model involves a series of nodes interconnected via links, where a water balance is satisfied at each node. Once the model is implemented, it is necessary to verify its capability for replicating the real environment through a calibration process. Calibration consists of adjustment of unknown or partially known parameters, in such a way that model outputs fit the observations. Because of its flexibility, robustness, and reliability for dealing with complex models, Bayesian Monte Carlo is chosen to perform such a task. This method updates statistically available knowledge

about parameters with the information in observed data. And most importantly, it is capable of assessing the effect of parameters on model predictions.

Since simulation models imply a combination of mathematical relationships describing some features of the nature, parameter estimates are prone to uncertainty. This parameter uncertainty has to be quantified to evaluate confidence limits on model response, so that model results are meaningful. The p-factor (percentage of observations bracketed by the uncertainty bands) and the r-factor (thickness of the uncertainty band) are used to accomplish this task.

1.2. Research Objectives

The specific objectives of the present study are as follows:

- development of distribution model for Punjab Irrigation System, describing its components and water routing mechanisms,
- calibration and validation of the proposed distribution model,
- uncertainty quantification of model parameters,
- correlation among model parameters.

The distribution model is expected to be useful to assist decision-makers in meeting the objectives of maintaining an equitable water distribution and maximizing water utility.

2. Literature Review

2.1. Modeling Framework

Water is one of the most crucial resource for human life on Earth. This essential element affects almost all sectors of the economy, such as agriculture, industry, energy production, and household water supply. The volume of freshwater in the world represents only 2.5% of total stock, and just 0.26% of global freshwater is accessible for human beings [2]. Due to global warming, population growth, and industrialization the quality and availability of freshwater is under threat, particularly in many developing countries such as Pakistan.

Climate change phenomena is likely to aggravate the water availability with a similar increase in irrigation water demand by 20 times until 2050 [3]. In that context, instabilities in agricultural production will negatively affect food security and the whole economy in the near future. Out of multiple strategies, a clever alternative to alleviate increasing water scarcity in agriculture is for instance an optimization of the irrigation systems through efficient technologies and planning tools.

Quantification of water resources and their seasonal variability is a key element of river basin models. These models are capable to simulate the spatial and temporal distribution of water resources, being able to handle complex operating rules and regulations into the system. A common feature of such models is the computation of water balance in each point of interest and time step. The model structure comprises a series of nodes interconnected via links, in which a water balance at each node is performed [4].

2.1.1. Node-link network structure

River basin model can be visualized as a series of nodes interconnected by links. Each node represents an inflow, diversion point of canals, or reservoirs. Links are longitudinal connections between nodes, that could represent rivers and demand canals [5]. The main attributes for links are the time lags and loss/gain coefficients. Typically, these attributes are used as parameters for model calibration [4].

2.1.2. Comparison of network models

The most commonly used network models in water resource management are MIKE HYDRO Basin, eWater Source, and WEAP. The summary of such network models is

given in Table 2.1. These comparisons do not discuss all the features of each model, rather provide a general impression of the capabilities and limitations built into such models.

Table 2.1.: Comparison of network models.

Model	**MIKE HYDRO Basin**	**WEAP**	**eWater Source**
Usage	Water availability, infrastructure planning, multisectoral demands, regulation i.e. water rights, priorities, water quality	Adaptive agriculture practices, canal linings, changes in reservoir operations, water conservation, water use efficiency	System operation, integrated planning from urban to river basin scale, lag and loss computations, suitable for IWRM studies
Ease of use	Relatively easy to use if user is familiar with ArcView software	Relatively easy to use, but requires significant data for analysis	Moderate
Key inputs	Water demand, water supply, hydropower, reservoir information: water quality	Water demand, water supply, scenarios, pollution changes, socioeconomic projections, water supply projections	Historic flows at inflow nodes, reservoir operation details, demand at canal heads and for the account holder
Key outputs	Hydrologic volume and flow descriptions throughout the system, water diversions, water quality of dissolved solids and temperature	Mass balances, water diversions, water use: benefit/cost scenarios	Flow hydrographs at different nodes and canal heads
License	Paid (both Mike Basin as well as Arc View)	Paid with free upgrade	Paid, limited versions are free
Code language	VB, Python, C++	Automation Server i.e other languages Java and Python can directly control WEAP	Unknown

Source: [6].

2.2. Bayesian Model Framework to Uncertainty Estimation

Bayesian Theorem is a statistical approach to perform stochastic calibration, where current knowledge about a parameter is updated with observed data. In general, the Bayes workflow relies on a definition of prior distribution capable of handling the available knowledge about the given scientific problem. Afterward, the likelihood function is determined using information about the observed data; and the combination of both prior and likelihood function gives as a result the posterior distribution. This expresses the updated knowledge given the observed data and prior beliefs [7]. The general form of Bayes Theorem is given below:

$$p(\theta \mid q) = \frac{p(q \mid \theta)\, p(\theta)}{p(q)} \tag{2.1}$$

where,

$p(\theta \mid q)$ is the posterior distribution. In order to perform stochastic calibration, Bayesian updating is used. Under such condition θ represents the hydrological model parameter and q is the observed data. $p(\theta)$ is the prior probability, which reflects the beliefs of the parameter values before observing data. $p(q|\theta)$ is the likelihood or conditional probability of observed data given the parameter θ. $p(q)$ is the marginal likelihood or Bayesian Model Evidence. This term is used as normalizing constant and only depends on observed data. In practice, $p(q)$ is not essential to estimate the posterior; thus, Bayes Theorem is often expressed as shown below:

$$p(\theta \mid q) \propto p(q \mid \theta)\, p(\theta) \tag{2.2}$$

2.2.1. Prior distribution

Prior distribution $p(\theta)$ is an important component of the Bayesian Theorem. It is expressed as Probability Density Function (PDF), either as uniform, normal, Poisson, among others. Most of the time, this distribution is based on information from previous studies and expert knowledge. According to the level of uncertainty in the model parameter, the prior is classified as informative, weakly informative, and diffuse [8]. Informative prior reflects a high certainty about the model parameter. In a normal distribution, it implies small variance surrounding the mean. Weakly informative prior has a regular certainty about the parameter. Consequently, it has larger variance and less impact in posterior results, owing to some assumption about the parameters [9]. Finally, diffuse prior conceptually shows a high uncertainty surrounding the parameter, where all values within the range are equally likely. Therefore, the observed data will essentially determine the posterior results [8]. Usually, there is vague knowledge or even a lack of information about the parameters. To overcome such issues, researchers suggest the use of uniform distribution with lower and upper limits expressing the plausible value ranges [10].

2.2.2. Likelihood distribution

Likelihood $p(q|\theta)$ is the conditional probability distribution given the model parameter θ, where the main purpose is to convey information about unknown quantities. In turn, the likelihood function summarizes the difference between the observed and simulated model, indicating the overall behavior assumed for measurement error or residuals. In general, the measurement error is assumed to be normally distributed ($\epsilon(t) \sim N(0, \sigma_0^2)$) and uncorrelated in time [11]. The Gaussian likelihood function then takes the following expression:

$$p(q|\theta, \sigma^2) = \prod_{i=1}^{n} \frac{1}{\sqrt{2\pi\sigma_i^2}} \exp\left[-\frac{1}{2} \frac{\sum_{j=1}^{n} \left(q_{ij}^{obs} - q_{ij}^{sim}(\theta) \right)^2}{\sigma_i^2} \right] \tag{2.3}$$

where q_{ij}^{obs} are the observed variables, $q_{ij}^{sim}(\theta)$ are the corresponding simulated responses given the parameter θ, and σ^2 refers to the variances of the simulation errors. This likelihood equation allows consideration of heteroscedasticity (variance depending on the information magnitude) of the data set [12].

2.2.3. Posterior distribution

The posterior distribution $p(\theta \mid q)$ describes the state of knowledge and uncertainty about the values of unknown parameters after observing the data. Therefore, the observed data set is a conditioning variable for posterior. In order to communicate the final results, the posterior distribution is summarized in form of mean, median, and credible intervals [13]. Due to the complex nature of the real systems and their models, this task is sometimes difficult to address by using equations or analytical solutions. Thus, iterative approaches based on Monte Carlo simulations are commonly used [14].

2.2.4. Data conditioning

Oftentimes, data set used in hydrological modeling needs a preprocessing step because residuals between predicted and observed values are heteroscedastic (unequal variance of the residuals over a range of measured values) [15]. In order to understand this concept lets consider the following linear regression:

$$yi = Xi\beta + \epsilon i,\ i = 1, ..., n \tag{2.4}$$

where yi represents the dependent variable, Xi is 1 x p vector of predictors, β is p-dimensional column vector of coefficients, and ϵ is the column vector of error. One assumption of Ordinary Least Squares is that variance of ϵ is constant; however, it is not always true in practice, leading to heteroscedasticity of the error variance [16]. During the calibration of parameters in hydrological models, one assumption is that

model residuals follow a Normal distribution with constant variance and zero mean [17]. Under this supposition, the model residual is defined as:

$$\epsilon(t) = q_{sim}(t) - q_{obs}(t), \text{with } \epsilon(t) \sim N(0, \sigma_0^2) \tag{2.5}$$

where t refers to time and σ_0^2 is a constant error variance.

Researchers suggest that heteroscedasticity is a natural phenomenon in hydrological systems [18]. Therefore, it is important to analyze quantitatively the heteroscedasticity of model residuals and perform variance stabilizing techniques. Heteroscedastic testing has been widely investigated, starting from informal diagnostics such as scatter plots to the most sophisticated statistical tests. Visual inspection is only helpful to suggest the presence of heteroscedasticity, the next step should be the verification of such concerns by using formal tests [19]. Formal statistical tests such as Breusch Pagan (1979), White (1980), and Su and Ullah (2013) have been used to examine whether the residuals are correlated or not.

To stabilize the variance of the residuals, and thus mitigate heteroscedasticity, Box-Cox transformation can be applied to observed and simulated data[20]:

$$q'_{obs} = \begin{cases} \frac{q_{obs}^{\lambda}-1}{\lambda} & \text{if } \lambda \neq 0 \\ \log q_{obs} & \text{if } \lambda = 0 \end{cases} \quad \text{and} \quad q'_{sim} = \begin{cases} \frac{q_{sim}^{\lambda}-1}{\lambda} & \text{if } \lambda \neq 0 \\ \log q_{sim} & \text{if } \lambda = 0 \end{cases} \tag{2.6}$$

where q'_{obs} and q'_{sim} are the transformed observed and simulated data, respectively. λ is the Box-Cox parameter. Now, the transformed model residual becomes:

$$\epsilon(t)' = q_{sim}(t)' - q_{obs}(t)' \tag{2.7}$$

2.3. Assessing Model Performance

The model performance during calibration and validation is quantified by comparing simulated flows with corresponding observed flows. The coefficient of determination (R^2) is a test which evaluates the linear dispersion between observations and simulations, it describes the variance in the observed data that is explained by the model [21]. R^2 interval is between 0 and 1, where values closer to 1 indicate better agreement or less error variance, and usually values larger than 0.5 are considered as acceptable [22]. The definition of R^2 can be seen in the following equation:

$$R^2 = \left(\frac{\sum_{i=1}^{n}(q_i^{obs} - \mu_{obs})(q_i^{sim} - \mu_{sim})}{\sqrt{\sum_{i=1}^{n}(q_i^{obs} - \mu_{obs})^2}\sqrt{\sum_{i=1}^{n}(q_i^{sim} - \mu_{sim})^2}} \right)^2 \tag{2.8}$$

where μ_{obs} and μ_{sim} represent the mean of observed and simulated values, respectively.

One of the major drawbacks of R^2 is the fact that only the linear dispersion between the observed and predicted value is evaluated, ignoring variations of minimum and maximum values [23], therefore a conjunctive use of R^2 with other indicators is suggested. The Nash–Sutcliffe Efficiency (NSE, Nash and Sutcliffe, 1970) is the most popular criterion to evaluate the goodness-of-fit of hydrological models. NSE is a dimensionless goodness-of-fit index that evaluates the Mean Square Error (MSE) of observed and simulated data (noise), compared to the variance in the measured value [21]. This indicator is commonly the measure of choice for evaluating model performance because it normalizes the MSE into the most interpretable way [24]. The NSE is calculated as shown in the following equation:

$$NSE = 1 - \frac{\sum_{i=1}^{n}(q_i^{obs} - q_i^{sim})^2}{\sum_{i=1}^{n}(q_i^{obs} - \mu_i^{obs})^2} \tag{2.9}$$

where n is the number of time-steps. NSE values can vary from $-\infty$ to 1 and generally falls within 0 to 1 unless there are severe errors in the used data [25]. As usual, a NSE $= 1$ indicates a perfect agreement between observed and simulated discharges; while NSE < 0 suggests that the observed mean is a better predictor than simulation itself. And NSE $= 0$ implies that simulated model has the same performance as the mean of observed data, that means results in overall are reliable, but under the assumption that errors during simulation are considerable [26]. Generally, the reference values of NSE performance are classified as follows: < 0.5 as inadequate, $0.5 - 0.6$ as fair, $0.65 - 0.75$ as good, and > 0.75 as very good [27], [28], [29].

Even the fact that NSE is one of the recommended indicators for model performance, some limitations should be taken into account [30], namely its high sensitivity to peak flows in model calibration which is due to the squared differences in formulating this indicator. Moreover, NSE is susceptible to larger model residuals, due to the heteroscedasticity phenomena in high flows [31].

Kling-Gupta Efficiency (KGE, Gupta et al. 2009) is a decomposition of NSE which addresses its several shortcomings such as the problematic interplay between the linear correlation and flow variability error [32]. The KGE combines the correlation, variability bias, and mean bias which are components of the mean square error [33]. In general, a value of ≥ 0.50 is used as a threshold for the daily time step of hydrological models [29]. This indicator is defined as shown below:

$$KGE = 1 - \sqrt{\left(\frac{\mu_{sim}}{\mu_{obs}} - 1\right)^2 + \left(\frac{\sigma_{sim}}{\sigma_{obs}} - 1\right)^2 + (r-1)^2} \tag{2.10}$$

where σ_{obs} is the standard deviation of observed values and σ_{sim} the standard deviation of simulated values (measure of variability). The μ_{obs} and μ_{sim} express the bias error. And r is the linear correlation coefficient between simulated and observed values which can lie between -1 to +1.

Percent bias (PBIAS) is the deviation of streamflow discharge expressed as a percentage, it indicates the simulated data to be larger or smaller than the observations. Negative values suggest the model toward underestimation (underprediction), whereas positive values mean model overestimation (overprediction). Its value ranges from $-\infty$ to $+\infty$, with low magnitudes indicating high model accuracy [34]. PBIAS is calculated as a percentage as shown in the following Equation:

$$PBIAS = 100 * \left[\frac{\sum_{i=1}^{n} (q_i^{obs} - q_i^{sim})}{\sum_{i=1}^{n} (q_i^{obs})} \right] \tag{2.11}$$

PBIAS values tend to be more sensible during dry years than wet years; therefore, this fact should be contemplated when splitting the sample for calibration and validation [34]. In general, PBIAS$+/-25\%$ is considered as satisfactory value for daily time step calibration of hydrological models [35].

The Table 2.2 shows a summary of the discussed model performance indicators:

Table 2.2.: Summary of model performance criterion.

N°	**Performance criteria**	**Description**	**Threshold**
1	R^2	Linear dispersion between observations and simulations	>0.60
2	NSE	Mean square error (MSE) of observed and simulated data (noise), compared to the variance in the measured value	>0.50
3	KGE	Decomposition of the NSE, which helps to analyze the importance of its different components (correlation, bias, and variability).	≥ 0.50
4	PBIAS	Indicates the simulated data to be larger or smaller than the observations	+/-25%

3. Methodology

3.1. Study Area

The area under study corresponds to Punjab province, Pakistan (Figure: 3.1). Punjab is the epicenter of agriculture being the largest producer of major crops around Pakistan. However, about 78% of total available water is used for irrigation [1], making the primary consumer of water resources among other provinces [36]. In this way, Punjab province is home to the more complex Indus Basin Irrigation System (IBIS), reportedly the largest contiguous hydraulic infrastructure in the world [1]. The IBIS is fed by Indus and Chenab rivers from the West, and Sutlej, Ravi, and Beas tributaries from the East [37].

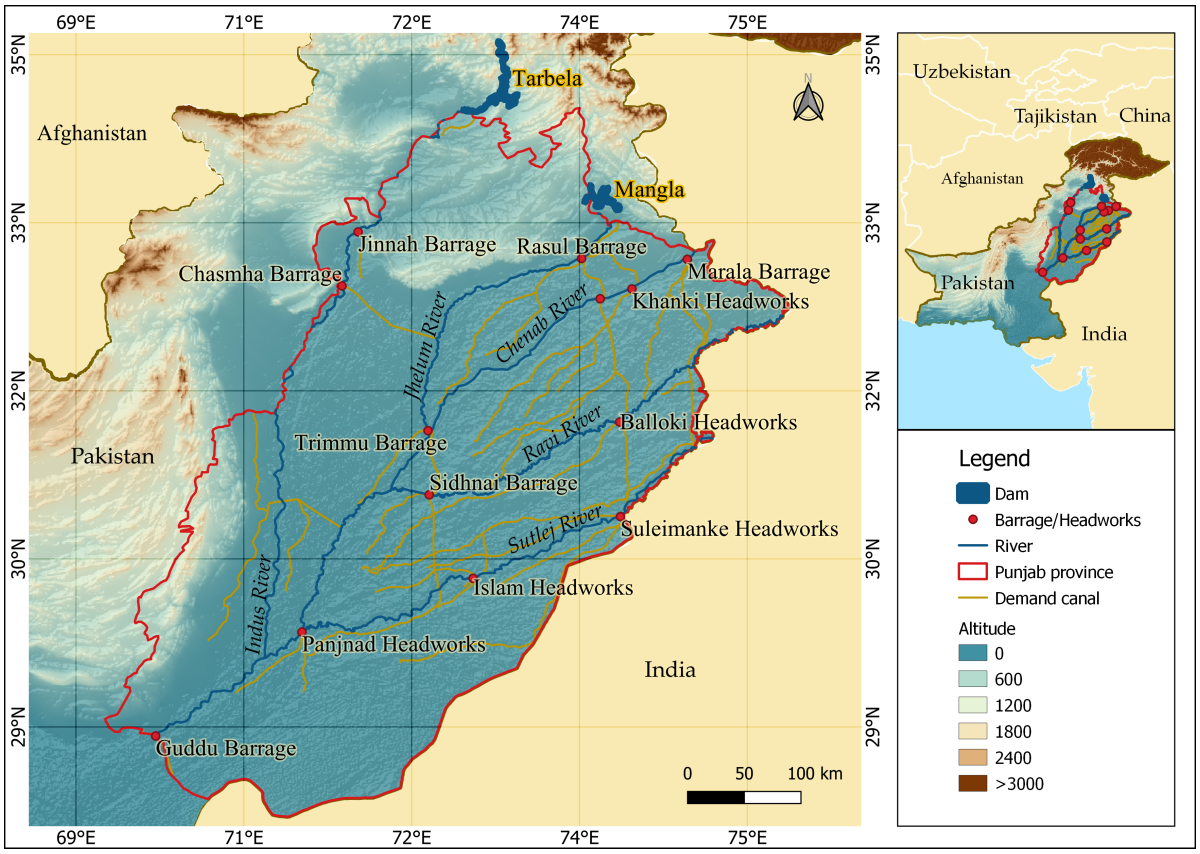

Figure 3.1.: Location of the study area.

The irrigation system in Punjab comprises 13 barrages, 2 siphons across the Ravi and Sutlej rivers, 12 interlinked canals, and 23 major canals [38]. The Indus river conducts water from Tarbela Dam to Jinnah, Chasma, and Taunsa headworks, which also connects to two link canals. Similarly, the Jhelum river provides surface water from Mangla Dam to Rasul, which feds two major canals. The Chenab river delivers water to Marala, Khanki, Qadirabad, and Trimmu barrage, which on the way feds four irrigation canals and five links. Finally, the Ravi river supplies surface water to Balloki and Sindhnai headworks and the Sutlej river to Sulemanki, Islam, and Punjnad barrage. The schematic diagram of the Punjab Irrigation System including the reservoirs, barrages/headworks, links, and main canals is shown in Figure 3.2.

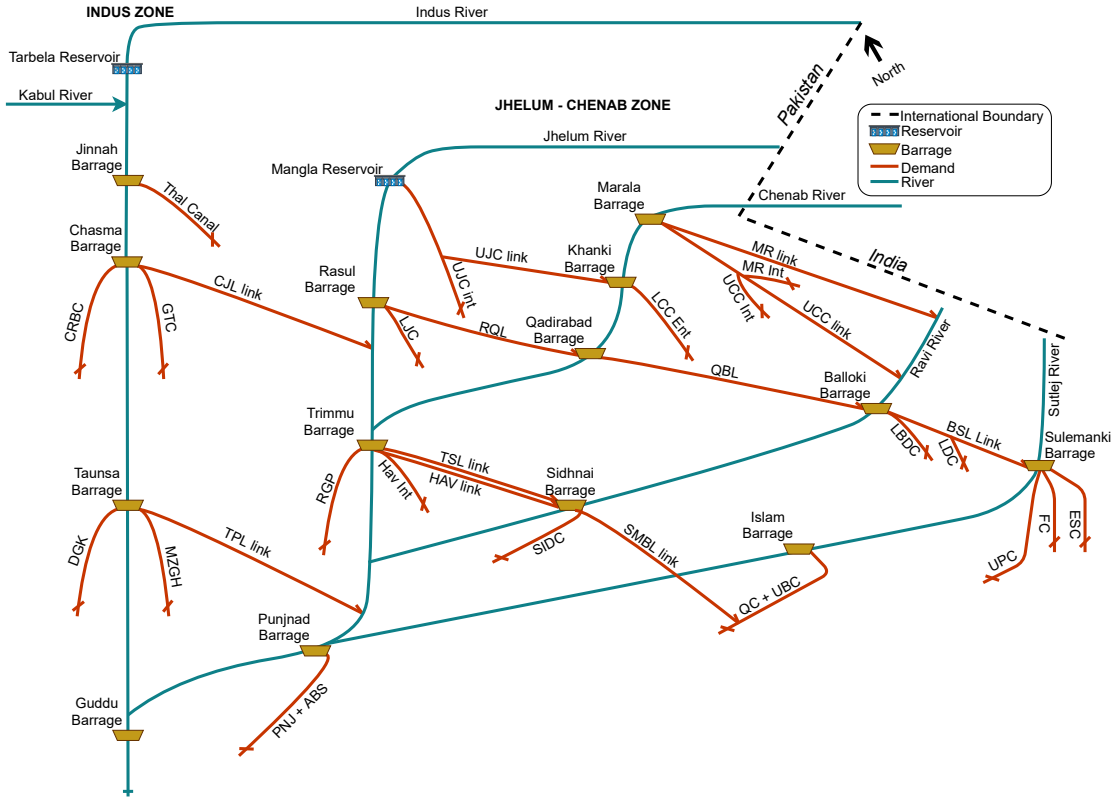

Figure 3.2.: Schematic diagram of Punjab Irrigation System showing rivers, barrages, major and link canals taking off from barrages.

The Punjab irrigation canals are stretched across 36,862 km length covering 9.70 Mha. According to the Water Appointment Accordance of 1991 (IRSA 1991), Punjab province is entitled to 56 MAF (11964.8 MCM) of surface water. Out of the total, about 37.5% of water is lost during distribution and conveyance from river heads to canals, just before reaching the crop fields. Furthermore, percolation, leaching, evapotranspiration, and run-off losses represent about 25% of total water. In consequence, only the remaining 37.5% of water is available for crops [39].

In this scenario, equitable and sustainable distribution of water turns more difficult being a matter of concern for the decision-makers in the water sector. To summarize, there is a need to characterize the entire Punjab Irrigation System by taking into account all the constraints and its elements (dams, barrages/headworks, main and link canals). Thus, suggest efficient strategies for distributing the surface irrigation water. Keeping in view the operational complexities of the water supply system in Pakistan, the above-discussed models (Table: 2.1) could not be capable to handle such a complex system with the demand-based operation and provincial water rights. As an alternate modeling tool, a flexible node-network model is adopted in this study.

The first part of this thesis addresses the development of a distribution model and the second part focuses on calibration, validation, and uncertainty quantification of parameters through the Bayesian Monte Carlo method.

3.2. Data Requirement and Source

To characterize the Punjab Irrigation System through a distribution model, good quality of the data set needs to be ensured. Inputs about daily discharge data, link canals, demand canals, and dams are mainly required for model development. Historical data from April 1, 2011 to March 31, 2016, were obtained from Indus River System Authority (IRSA), Project Monitoring and Implementation Unit (PMIU), Indus Water Treaty (IWT): A directorate of PMIU, and Punjab Irrigation Department (PID).

3.3. Network Model

The procedure for the model development consists of three main components. The first component refers to model inputs and pre-processing, the second part focuses on the structure and model simulation itself, and the third component involves the model post-processing in terms of calibration and uncertainty quantification of the parameters.

3.3.1. Model inputs

Barrages/headworks and dams

All the barrages/headworks and dams depicted in Table 3.1 are used as model inputs. It is important to emphasize that water balance is performed at each node.

Major and link Canals

Similarly, major and link canals are incorporated as inputs in the distribution model (Table 3.2). Each link canal has a maximum design capacity, which is a main constraint in the model.

Table 3.1.: Barrages and headworks in the Punjab surface water flow model.

Category	River	Name	Node
Barrage	Indus	Jinnah	JIN
Barrage	Indus	Chasma	CHS
Barrage	Indus	Taunsa	TNS
Barrage	Jhelum	Rasul	RSL
Barrage	Chenab	Marala	MRL
Barrage	Chenab	Khanki	KNK
Headwork	Chenab	Qadirabad	QBD
Headwork	Chenab	Trimmu	TRM
Barrage	Chenab	Punjnad	PNJ
Headwork	Ravi	Balloki	BLK
Barrage	Ravi	Sidhnai	SID
Headwork	Sutlej	Sulemanki	SUL
Headwork	Sutlej	Islam	ISL
Dam	Indus	Tarbela	TRB
Dam	Jhelum	Mangla	MNG

Time lags

The primary information source for the time delays is taken from PID. However, in this study different values have been explored manually to check the accuracy of the time lags. These lag values are based on a daily time step; that is, the full day is considered only if travel time is more than 12 hours otherwise, no time lag is taken. Afterward, the time lags between two nodes are incorporated to simulate the dynamics of water flow routing in river reaches and link canals. The Table 3.3 shows the values used in the model.

3.3.2. Model development

The entire distribution model was developed by using MATLAB programming software. The model structure of the Punjab Irrigation System involves a series of nodes connected through links, where the principle of water balance is performed at each node, in such a way that water flowing in should be equal to water flowing out plus gains/losses. The series of nodes represent either storage dams or barrages/headworks (junctions). Similarly, the interconnected links physically represent the river reaches, links, and main canals. The time-lag and gain/loss coefficients are regarded as the main attributes of these links, the latter is used as calibration parameters. The combination of links and the series of nodes gives a final structure of the network flow model. The Figure 3.3 shows a part of the model structure, wherein water is routed towards the Punjnad demand node through the TPL link and river reaches. The source nodes are Trimmu, Sidhnai, Islam, and Taunsa. In this way, the off-taking canals at each node can get water either from river reach or link canals.

Table 3.2.: Major, internal and link canals in Punjab Irrigation System.

Category	River	Name	Node	Capacity (m^3/s)
Link canal	Indus	Chasma - Jhelum	CJL	614
Link canal	Indus	Taunsa - Punjnad	TPL	340
Link canal	Jhelum	Upper Jhelum Canal	UJC	170
Link canal	Jhelum	Rasul - Qadirabad	RQL	538
Link canal	Chenab	Upper Chenab Canal	UCC	100
Link canal	Chenab	Marala - Ravi	MRL	594
Link canal	Chenab	Qadirabad - Balloki	QBL	623
Link canal	Chenab	Trimmu - Sidhnai	TSL	340
Link canal	Ravi	Balloki - Sulemanki	BSL	595
Link canal	Ravi	Sidhnai - Maiulsi - Bhawal	SMBL	340
Major canal	Indus	Thal canal	THAL	255
Major canal	Indus	Chasma Right Bank	CRBC	51
Major canal	Indus	Greater Thal Canal	GTC	113
Major canal	Indus	D.G Khan Canal	DGK	252
Major canal	Indus	Muzaffargarh Canal	MZGH	235
Internal canal	Jhelum	Upper Chenab Internal	UCC int	396
Major canal	Jhelum	Lower Jhelum Canal	LJC	184
Major canal	Jhelum	Rangpur Canal	RGP	76
Major canal	Jhelum	Haveli internal canal	HAV int	40
Major canal	Ravi	Sidhnai Canal	SIDC	1274
Major canal	Chenab	Lower Chenab Canal	LCC	348
Internal canal	Chenab	Marala Internal Canal	MR int	51
Major canal	Ravi	Lower Bari Doab Canal	LBDC	258
Major canal	Ravi	Lower Depalpur Canal	LDC	119
Major canal	Sutlej	Eastern Sadiqia Canal	ESC	164
Major canal	Sutlej	Fordwah Canal	FC	96
Major canal	Sutlej	Upper Pakpattan Canal	UPC	159
Major canal	Sutlej	Upper Bhawal and Qaim	QC-UBC	91
Major canal	Jhelum	Punjnad - Abbasia	PN+AB	14158

Gain/loss coefficient estimation

In the distribution model, the conveyance gains and losses take place within the river reaches and link canals. A simple linear regression between two nodes was used to estimate these gain/loss coefficients in such a way that flow routing is simulated in each section. Those values are used as calibration parameters in the modeling system.

In Figure 3.3, Punjnad upstream is considered as a dependent variable, whereas the source nodes (Taunsa, Trimmu, Sidhani, Islam) are assumed as independent variables. In case, there is only one source node (e.g. Mangla to Rasul), a simple linear regression between the nodes is applied. Similarly, if there are two or more source nodes, multiple linear regression is applied. To calculate the coefficients of linear regression the following

Table 3.3.: Time lags in river reaches and canals

Reach and month wise lags													
Reach		**Months**											
From	**to**	**4**	**5**	**6**	**7**	**8**	**9**	**10**	**11**	**12**	**1**	**2**	**3**
Tarbela	Jinnah	2	1	1	1	1	1	1	1	1	2	2	2
Jinnah	Chasma	1	1	1	1	1	1	1	1	1	1	1	1
Chasma	Taunsa	4	3	3	2	2	2	2	2	2	4	4	4
Taunsa	Guddu	4	3	3	3	3	3	3	3	3	4	4	4
Mangla	Rasul	1	0	0	0	0	0	0	0	0	1	1	1
Rasul	Trimmu	5	4	4	3	3	4	4	4	4	5	5	5
Marala	Khanki	1	1	1	1	1	1	1	1	1	1	1	1
Khanki	Qadirabad	0	0	0	0	0	0	0	0	0	0	0	0
Qadirabad	Trimmu	5	4	4	3	3	4	4	4	4	5	5	5
Trimmu	Punjnad	7	6	6	5	5	5	5	5	5	7	7	7
Balloki	Sidhnai	9	8	8	7	7	8	8	8	8	9	9	9
Sidhnai	Punjnad	7	6	6	5	5	5	5	5	5	7	7	7
Sulemanki	Islam	4	3	3	2	2	3	3	3	3	4	4	4
Islam	Punjnad	8	6	6	5	5	5	5	5	5	8	8	8
Punjnad	Guddu	2	2	2	2	2	2	2	2	2	2	2	2
CJL head	Tail	2	2	2	2	2	2	2	2	2	2	2	2
TPL head	Tail	3	3	3	3	3	3	3	3	3	3	3	3
UJC head	Tail	2	1	1	1	1	1	1	2	2	2	2	2
RQL head	Tail	1	0	0	0	0	0	0	0	0	1	1	1
QBL head	Tail	4	3	3	3	3	3	3	3	3	4	4	4
BSL head	Tail	1	1	1	1	1	1	1	1	1	1	1	1
UCCL head	Tail	3	3	3	3	3	3	3	3	3	3	3	3
MRL head	Tail	3	3	3	3	3	3	3	3	3	3	3	3
TSL head	Tail	2	2	2	2	2	2	2	2	2	2	2	2
HAV head	Tail	2	2	2	2	2	2	2	2	2	2	2	2

equation was used:

$$y = mx \quad \text{or} \quad y = mx_1 + mx_2 + ...mx_n \tag{3.1}$$

where x is the independent variable, y is the dependant variable, and m is the slope coefficient corresponding to each x value.

Optimized flow paths, ranking and decision matrix

As mentioned earlier, there are various paths from where the demand for main canals is fulfilled. The algorithm to find the optimum flow path between the nodes consists of verifying the minimum loss factors in the given section. These loss coefficients are assigned according to the results of regression analysis. As an example, Figure 3.4 illustrates four source nodes that are feeding Sidhnai barrage. As shown, the path Balloki-Sidhani is the prioritized route in the ranking, which implies that the main

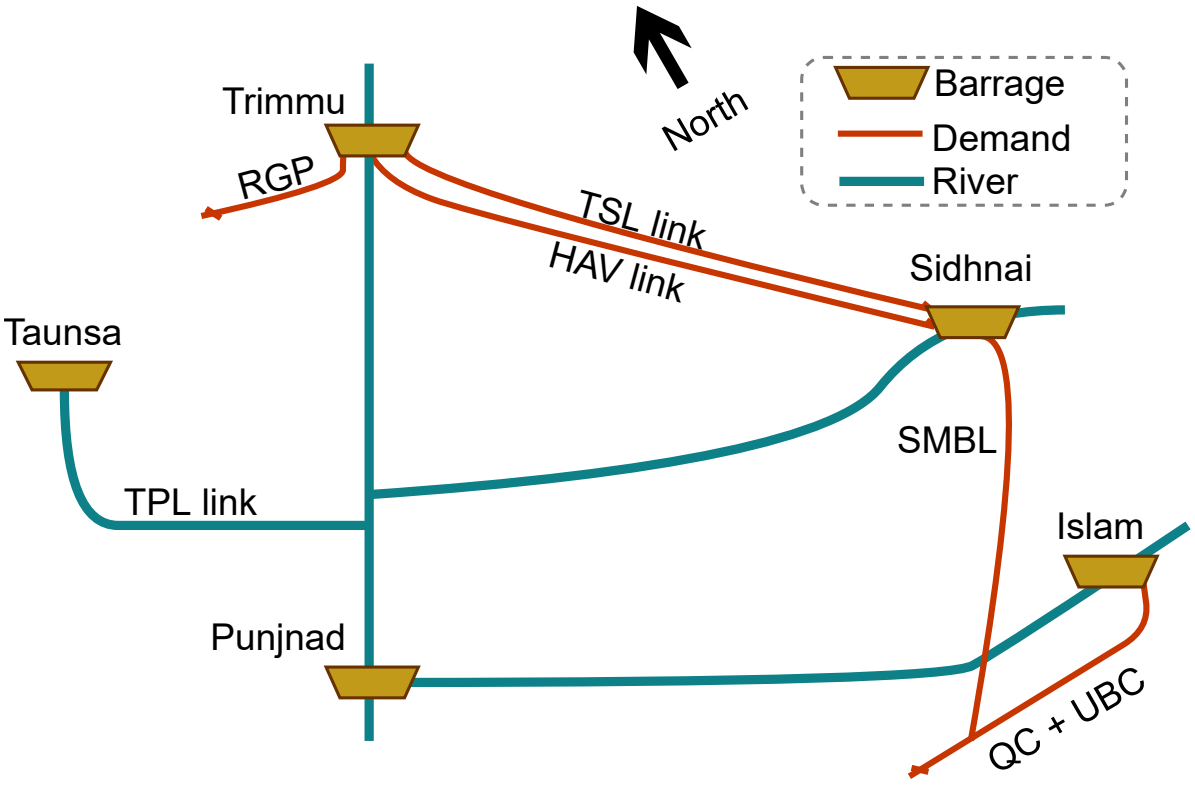

Figure 3.3.: Example of network structure with link canals, main canals, barrages and inflows at Punjnad node.

source of water supply for Sidhnai is Balloki barrage. Similarly, if Balloki's demand is not fulfilled yet, Trimmu barrage feds the water through TSL and HAV links. In this way, the Marala link provides water only if the demand with the main source has not been fully covered.

3.3.3. Calibration and validation

Model calibration involves finding suitable parameter values that best describe the natural system behavior. The regression parameters were calibrated for flow routing from the source nodes up to the demand nodes. In the framework of determining the good reliability of this complex system, Bayesian Monte Carlo method was applied since it is flexible, robust, and more suited for dealing with complicated problems. A schematic flowchart of the proposed Bayesian framework is shown in Figure 3.5.

About model extent, the simulation was performed from April 1, 2011 to March 31, 2016. From which, about two-third of the total discharge measurements were used for calibration and the remaining one-third for validation. In order to get an acceptable convergence, a total of $n_s = 100,000$ Monte Carlo realizations of parameters θ were performed.

In order to develop the Monte Carlo method for calibration, a set of prior vague knowledge about the gain/loss parameters was considered and represented by non-informative (diffuse) prior distributions. These uncertain coefficients were drawn from uniform distribution as several authors suggest. The upper and lower bounds between $U[0.7, 1.3]$ were chosen for all parameters based on the result of the preliminary regression analysis and because the given range covers both gain and losses equally. Additionally, defined lower and upper bounds consider almost one-third (30%) of the total discharge as losses or gains. It should be kept in mind that the calibration process was applied simultaneously in all river reaches (15) and link canals (10). Based on the scope of this study, the model only deals with the water distribution up to the head of the main canals. Hence, there is no need to address the system gains and losses from the main canal head up to the tail or farm level.

After an exploratory analysis of the residuals between simulations and observations, heteroscedasticity issues were identified as discussed in Section 2.2.4. To mitigate this problem, a Box–Cox transformation with parameter $\lambda = 0.001$ was applied to both measured q_{obs} and simulated q_{sim} discharge series:

$$q' = \frac{q^{\lambda} - 1}{\lambda} \tag{3.2}$$

Under the assumption of the required statistical hypotheses, such as normal distribution of measurement error, time independence of the residuals ($\epsilon(t) \sim N(0, \sigma_0^2)$, and homoscedasticity as explained in Section 2.2.4, the likelihood function takes the form:

$$p(q|\theta, u_i) = \prod_{i=1}^{n_s} \frac{1}{\sqrt{2\pi^{n_s}|R'|}} \exp\left[-\frac{1}{2}\left(q'_{sim} - q'_{obs}\right)^T R'^{-1}\left(q'_{sim} - q'_{obs}\right)\right] \tag{3.3}$$

in which n_s is the number of observations and R' expresses the $n_s \, x \, n_s$ covariance matrix of measurement errors with entries on the main diagonal, indicating that these values are uncorrelated.

Once the prior and the likelihood function is defined, the posterior of the model parameters were then estimated. The Rejection Sampling: filtration of prior via uniform distribution was applied since it is the most direct approach for determining the posterior. The main principle of this technique is to apply a correction form to the likelihood $p(q|\theta)$ by assigning weights w_i to each realization θ as shown below:

$$w_i = \frac{p(q|\theta)}{max(p(q|\theta))} \geq u_i \tag{3.4}$$

The likelihood realization is accepted as the ensemble of the posterior distribution if the weight w_i is greater or equal than the random number u_i, which is obtained from a uniform distribution $u(0, 1)$. The expression $max(p(q|\theta)$ is the maximum likelihood value from all n_s Monte Carlo realizations [40]. It is worth mentioning that the point in

the parameter range that maximizes the likelihood is named the Maximum Likelihood Estimate (MLE).

In reference to the model performance criteria, NSE>0.50, $R^2 > 0.60$, KGE$\geq$ 0.50, and PBIAS+/$-$25% were used as threshold values [35], [28], [29] as shown in Table 2.2 . NSE and R^2 were estimated with the help of MATLAB programming tool, correspondingly the KGE and PBIAS were calculated by using *HydroGOF* Rstudio package.

3.3.4. Uncertainty quantification

A reliable modeling approach must necessarily include quantification of its uncertainty. Within this framework, uncertainty assessment serves to verify the accurateness and preciseness of the proposed network model. Sources of uncertainty in hydrological models include errors in the input and output data, model definition, and parameter sets. Suitable analysis of these multiple uncertainty effects is still a big challenge. Due to the complex nature of the model, the uncertainty analysis in this thesis was focused on the impact of the parameters in the output discharges.

Uncertainty bounds were assigned by calculating the 2.5 and 97.5 percentiles from the posterior samples to generate a range with a 95% confidence level [41]. The uncertainties were quantified by $p-$ and $r-$factor indicators. The $p-$factor expresses the percentage of observations plus its error enveloped by the uncertainty bands and its value ranges from 0 to 1, where 1 implies total bracketing of the observed data by the given bounds (perfect simulation) [42]. In general, a value of $p-$factor>0.70 or 0.75 is recommended. But, it is subject to the project scale and input data [43]. On the other hand, $r-$factor measures the thickness of the envelope, and it is calculated as the ratio of the average width between the 2.5 and 97.5 percentiles and the standard deviation of the measurements. Its value varies between 0 and ∞, and usually, a limit of < 1.5 is acceptable [42], [43]. The p- and r-factors are closely dependant on each other, which suggests that a higher $p-$factor can be achieved only at the expense of a larger $r-$factor. Thus, a balance between both indicators has to be satisfied to generate acceptable calibrated parameters [44], [45]. The $r-$factor is described by the following expression:

$$r - factor = \frac{\frac{1}{n}\sum_{i=1}^{n}\left(y^{M}_{i,97.5\%} - y^{M}_{i,2.5\%}\right)}{\sigma_{obs}} \tag{3.5}$$

where $y^{M}_{i,97.5\%}$ and $y^{M}_{i,2.5\%}$ are the upper and lower uncertainty bands, respectively.

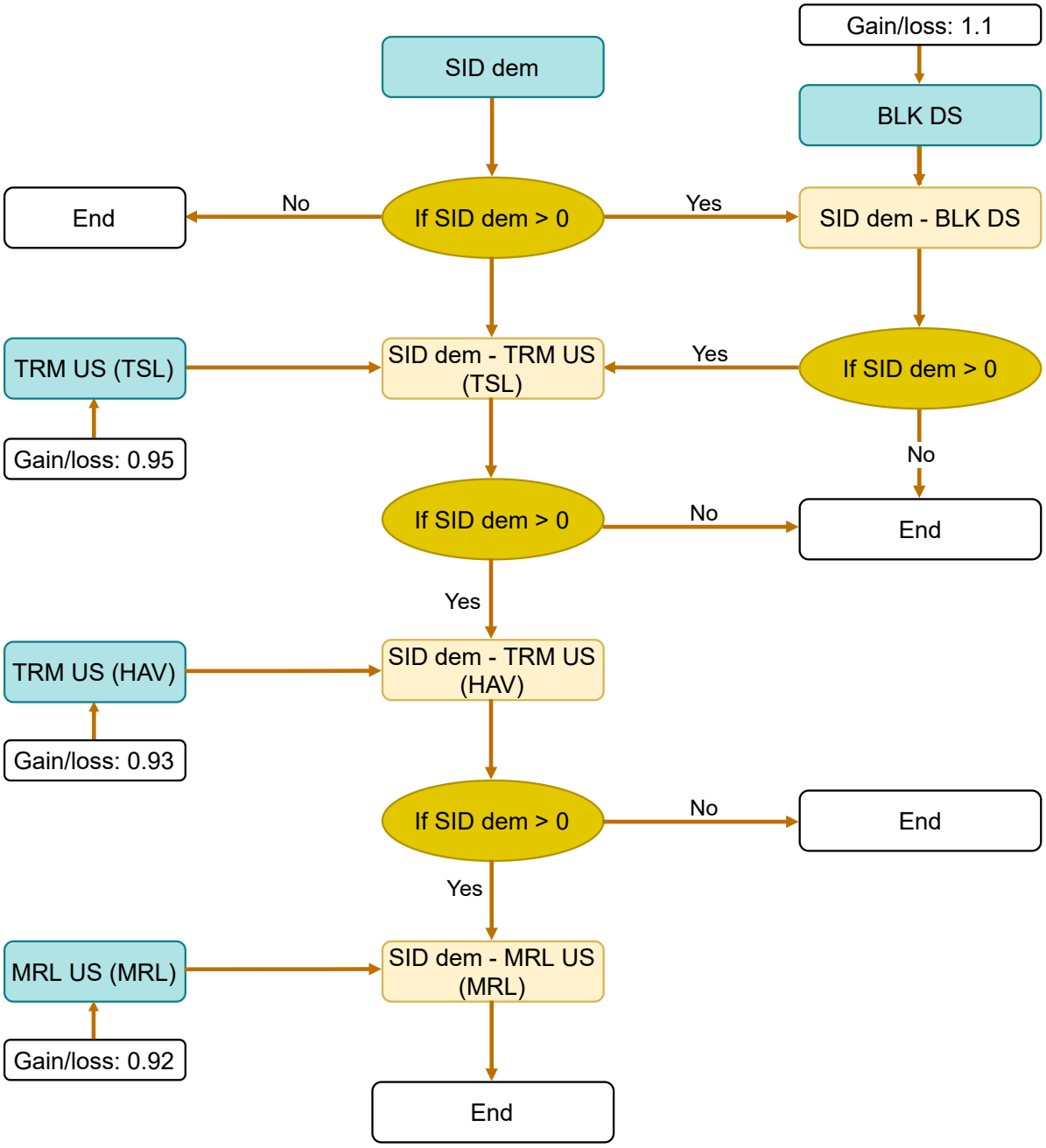

Figure 3.4.: Flow chart representing logic at Sidhnai node.

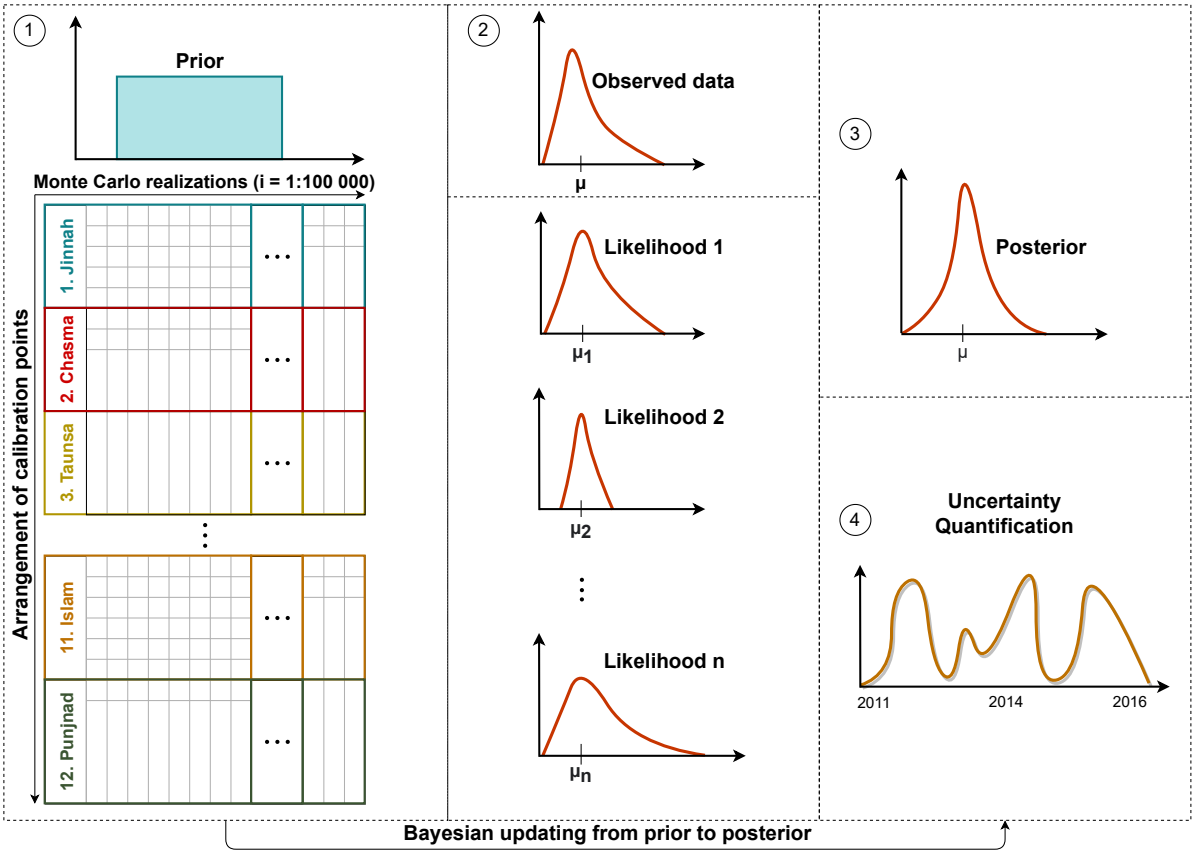

Figure 3.5.: Flow chart of Bayesian Monte Carlo framework. **1.** The workflow starts with definition of uniform prior $U[0.7, 1.3]$ and Monte Carlo realizations for all parameters. All barrage outflows are arranged in a single block to calibrate the model simultaneously. **2.** Probability Distribution Function of observed data and likelihood outputs. **3.** Output posterior distribution of model parameters and **4.** Uncertainty quantification.

4. Results

4.1. Calibration and Validation

The network model was simulated from April 1, 2011 to March 31, 2016. From which about two-third of the total discharge measurements were used for calibration and the remaining one-third for validation. To assess the simulation model performance, the calibration and validation were performed at the outflow or downstream of the 12 barrages/-headworks, which are distributed in the whole Punjab Irrigation System. The goodness-of-fit indicators, Nash-Sutcliffe Efficiency (NSE), Kling-Gupta Efficiency (KGE), Percent bias (PBIAS), and the coefficient of determination (R^2) are summarized in Table 4.1.

In the following, the results of the model performance are explained according to the statistical indicators. By taking a closer look at the model performance in terms of NSE, the Indus zone (Jinnah, Chasma, and Taunsa) presents high values, implying a good agreement between simulations and observations; while in Jhelum-Chenab zone, the NSE suggests moderate model behavior. But can still simulate the discharge with such accuracy. In Ravi and Sutlej zone, the model performance is still acceptable, except in Sidhnai barrage, where simulation is quite modest in both calibration and validation periods as shown by NSE = 0.48 and 0.40, respectively.

Concerning to KGE indicator, the obtained results are also satisfactory. In Indus zone, Jinnah barrage with KGE=0.89 and 0.92 is rather well simulated for both calibration and validation periods, respectively. Similarly, further south where Chasma and Taunsa barrages are located, the observations are quite well reproduced by the simulations. In Jhelum-Chenab zone, the simulated model captures with high accuracy the overall dynamics of the flow as indicated by the KGE. In Ravi and Sutlej zones, given the complexity of the system, KGE indicator still suggests a good simulation of discharge dynamics. Giving more attention to Islam barrage, the KGE implies that the calibration period (0.64) gives a higher model performance than the validation period (0.41).

The performance of the network model in terms of R^2 has as well satisfactory results, even taking into account that this indicator only evaluates the linear dispersion between observed and simulated discharges.

Finally, the PBIAS performance was satisfactory ($+/-25\%$) at most barrages, except for Chasma, Islam, and Punjand. The negative -26% and -30% of PBIAS at Chasma barrage suggest an underestimation of simulated flow. On the other hand, a positive PBIAS at Islam barrage indicates an overestimation of simulated discharge in both calibration and validation periods. Now, by exploring in more detail the model performance between

the irrigation zones, Western Indus, Jhelum, and Chenab performs better than Eastern Sutlej and Ravi river reaches.

Table 4.1.: Summary of model performance.

Barrage	Calibration				Validation			
	NSE	**KGE**	**PBIAS** [%]	R^2	**NSE**	**KGE**	**PBIAS** [%]	R^2
Jinnah ds	0.94	0.89	8	0.97	0.93	0.92	2	0.94
Chasma ds	0.76	0.58	-26	0.96	0.78	0.56	-30.2	0.95
Taunsa ds	0.86	0.72	-17.7	0.95	0.84	0.64	-23.8	0.94
Rasul ds	0.69	0.82	-2	0.75	0.82	0.78	18.8	0.84
Trimmu ds	0.72	0.83	-8.4	0.74	0.78	0.81	-16	0.80
Khanki ds	0.73	0.79	-1.8	0.73	0.63	0.73	-3.7	0.63
Qadirabad ds	0.78	0.78	19.2	0.80	0.68	0.82	8.1	0.72
Balloki ds	0.66	0.68	-21.8	0.68	0.62	0.69	-4.1	0.62
Sidhnai ds	0.48	0.72	-11.2	0.56	0.40	0.71	4.2	0.51
Sulemanki ds	0.86	0.83	-10.6	0.86	0.80	0.86	-6.5	0.81
Islam ds	0.78	0.64	34.9	0.80	0.64	0.41	56.9	0.75
Punjnad ds	0.75	0.65	30.3	0.76	0.71	0.80	-10.9	0.72

The optimized or calibrated parameters are shown in Table 4.2, where gains and losses are indicated among the river reaches and link canals. In the Indus zone, losses are high at the Jinnah-Chasma section (-25%), while there is a small net gain in the Tarbela-Jinnah and Chasma-Taunsa reaches. In the Jhelum zone, there is a 9% gain from Mangla to Rasul, but significant losses in the Rasul-Trimmu reach (-27%). In Chenab river, gains are quite high in the first two sections starting from Marala to Qadirabad; while in the section Qadirabad-Punjnad, considerable losses are observed. Correspondingly, in Ravi river losses are high in Sidhnai-Punjnad section. In Sutlej river, gains and losses are not significant compared to other rivers. Regarding the river links, most of them present considerable losses, only Taunsa-Punjnad (TPL), Marala link (MRL link), and Upper Chenab Canal (UCC) have +8%, -4%, and -5% gains/losses, respectively. The remaining link canals that take water from Jhelum, Ravi, and Sutlej rivers present high losses.

Finally, it is worth mentioning that there are two farming seasons in Pakistan named Kharif (April to September) and Rabi (October to March). In this way, supplementary information about the observed and simulated volumes for both seasons can be found in Appendix (Table A.3 and A.4) section.

4.2. Uncertainty Quantification

Figure 4.1, 4.2, and 4.3 show the time series plots of Maximum Likelihood Estimate (MLE), observed, and the Ensemble Mean from posterior sampling throughout the calibration and validation periods. The illustrations include as well the uncertainty band

Table 4.2.: Summary of calibrated model parameters.

River/link	Reach	Routing coefficient	Gain/loss (+/-)%
Indus	Tarbela - Jinnah	1.07	+7
Indus	Jinnah - Chasma	0.75	-25
Indus	Chasma - Taunsa	1.07	+7
Indus	Taunsa - Guddu	0.99	-1
Jhelum	Mangla - Rasul	1.09	+9
Jhelum	Rasul - Trimmu	0.73	-27
Chenab	Marala - Khanki	1.15	+15
Chenab	Khanki - Qadirabad	1.16	+16
Chenab	Qadirabad - Trimmu	0.75	-25
Chenab	Trimmu - Punjnad	0.70	-30
Ravi	Balloki - Sidhnai	1.13	+13
Ravi	Sidhnai - Punjnad	0.82	-18
Sutlej	Sulemanki - Islam	0.99	-1
Sutlej	Islam - Punjnad	1.01	+1
Sutlej	Punjnad - Guddu	0.96	-4
CJ link	Head to tail	0.94	-6
TPL link	Head to tail	1.08	+8
UJC link	Head to tail	0.72	-28
RQL	Head to tail	0.81	-19
MR link	Head to tail	0.96	-4
UCC link	Head to tail	0.95	-5
QBL	Head to tail	0.74	-26
TSL link	Head to tail	0.76	-24
HAV link	Head to tail	0.85	-15
BSL link	Head to tail	0.80	-20

at 2.5 and 97.5 percentiles for the cumulative probability distribution of the simulated discharges. By looking at the statistical p- and r-factors, at most of the barrages the model performance is "satisfactory" (p-factor>0.70 and r-factor<1.5) in both calibration and validation periods. In Indus zone, the uncertainties generally look large as illustrated by shaded regions. For instance in Jinnah barrage, values of p-factor=0.75 and r-factor=0.70 indicate large uncertainties during the validation period. Similarly, in Taunsa barrage values of r-factor=1.80 and 1.14 during calibration and validation periods suggest large uncertainties in the model. On the other hand, in Jhelum-Chenab zone, uncertainty bounds are quite tight compared with the Indus zone. For example, in Khanki barrage, the width of the uncertainty bounds is small as suggested by r-factor (0.42 and 0.23), although a few simulated data are bracketed within the given bounds as indicated by p-factor (0.75 and 0.67). In the case of Rasul barrage, there are relatively more uncertainties during calibration as expressed by low p-factor (0.73) and high r-factor (1.28). In Ravi and Sutlej rivers, the percentage of simulated discharges

bracketed by the given bounds are significantly acceptable, except in the Islam barrage where the p-factor for calibration was 0.67. Regarding the r-factor in Balloki, Sulemanki, and Islam barrages, the values indicate small width of the uncertainty bounds; while in Sidhnai barrage there is large uncertainty.

4.3. Correlation Between Model Parameters

Figure 4.4 shows the posterior probability distributions for the 15 river reach model parameters and 10 link canals. The proposed method accurately infers the given parameters and quantifies corresponding uncertainties. As indicated in the off-diagonal, the parameters show slight posterior correlations with each other. Along the main diagonal the kernel smoothing density shows the distribution of posteriors. These posterior distributions represent our uncertainty in the parameters after combining the information in the data and our prior beliefs. Based on this, Jhelum-Chenab zone (mng-rsl, mrl-knk, knk-qbd) shows the most probable parameter values accurately compared to other zones. Regarding the link canals, posterior rql, qbl, and bsl indicate the most likely values correctly.

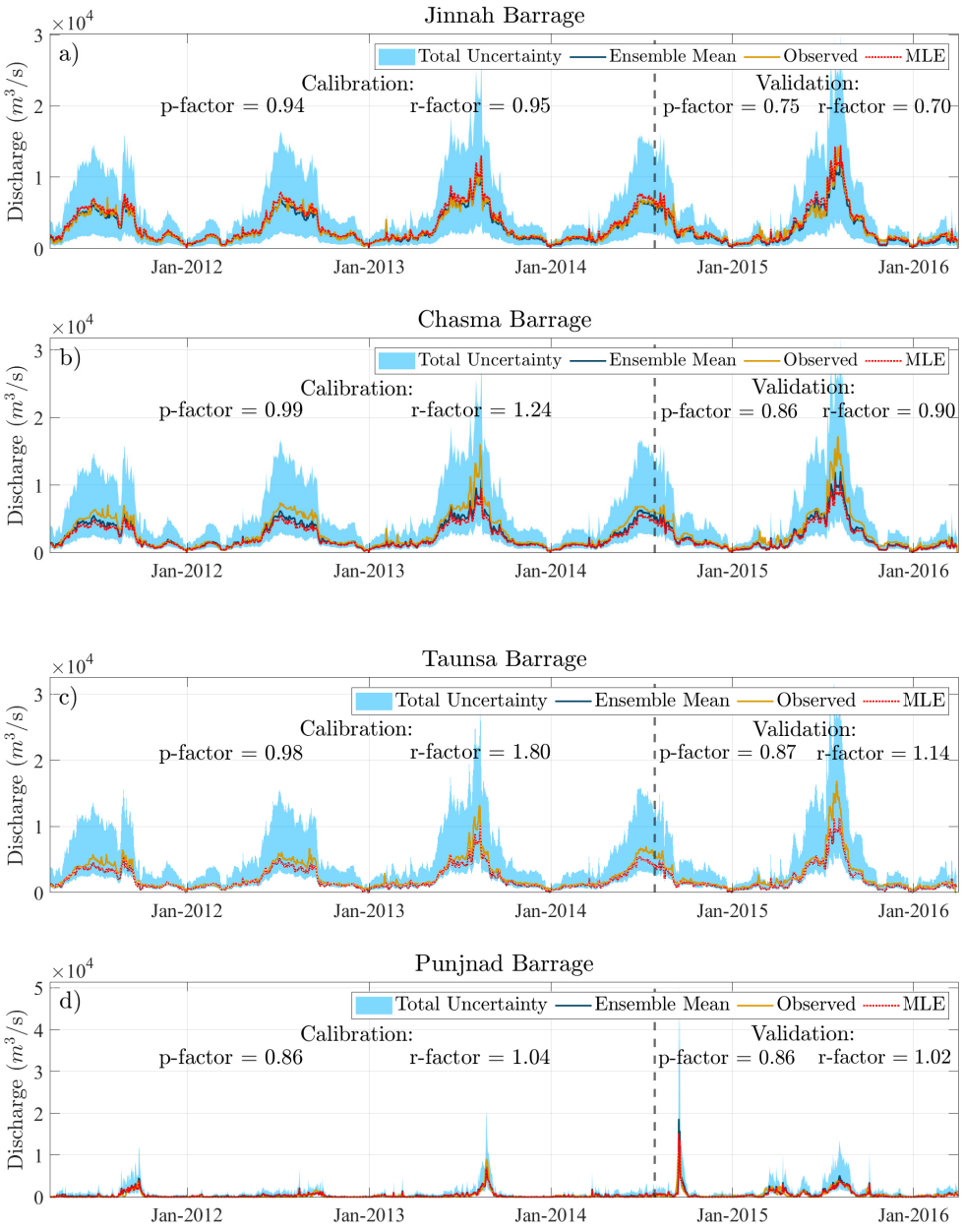

Figure 4.1.: Time series plot of Indus zone (a, b, c) and Punjnad barrage (d) including Maximum Likelihood Estimate (MLE), Ensemble Mean, and observed values. Uncertainty was defined by computing 97.5 and 2.5% levels of the cumulative distribution of the output variables.

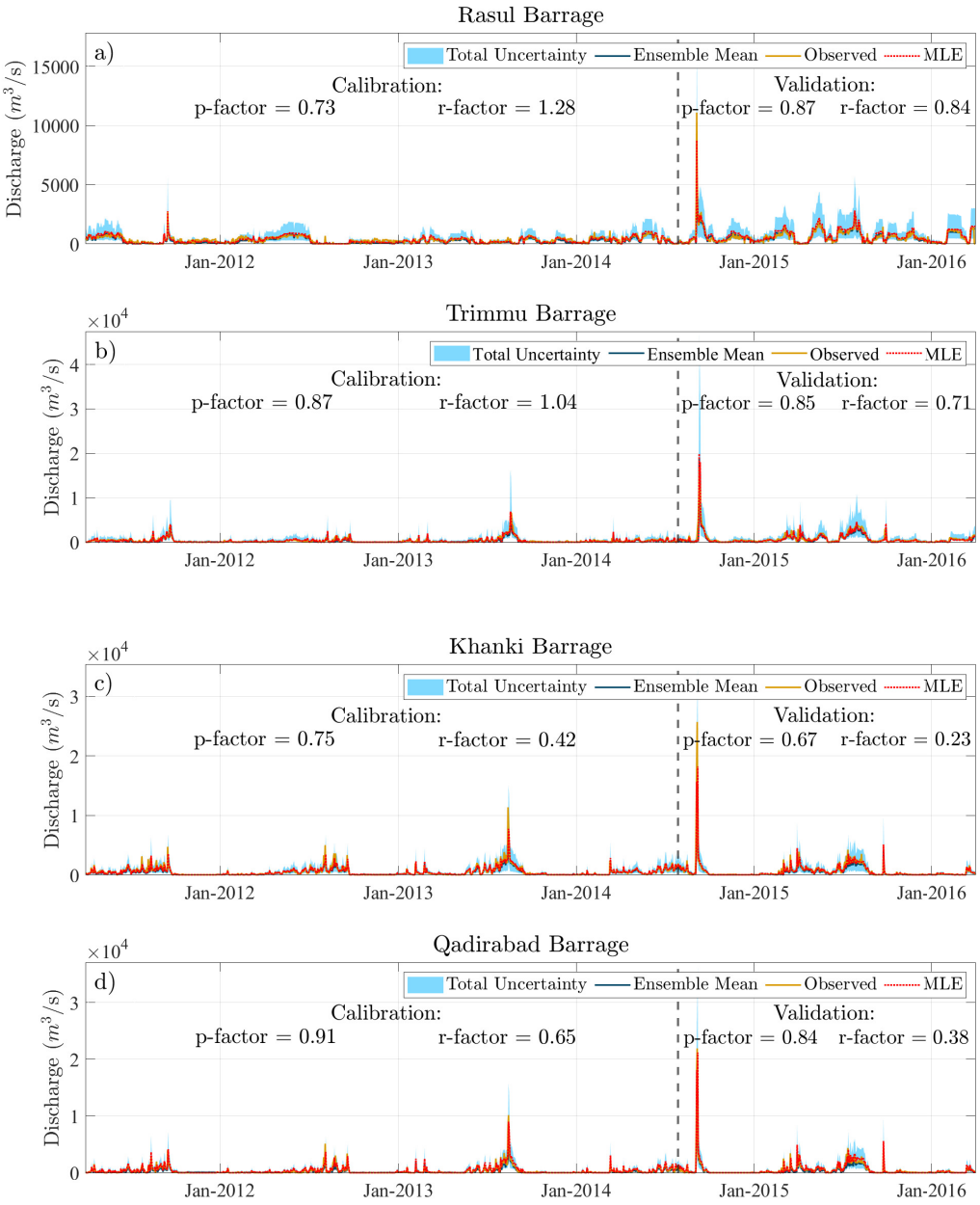

Figure 4.2.: Time series plot of Jhelum-Chenab zone (a, b, c, d) including Maximum Likelihood Estimate (MLE), Ensemble Mean, and observed values.

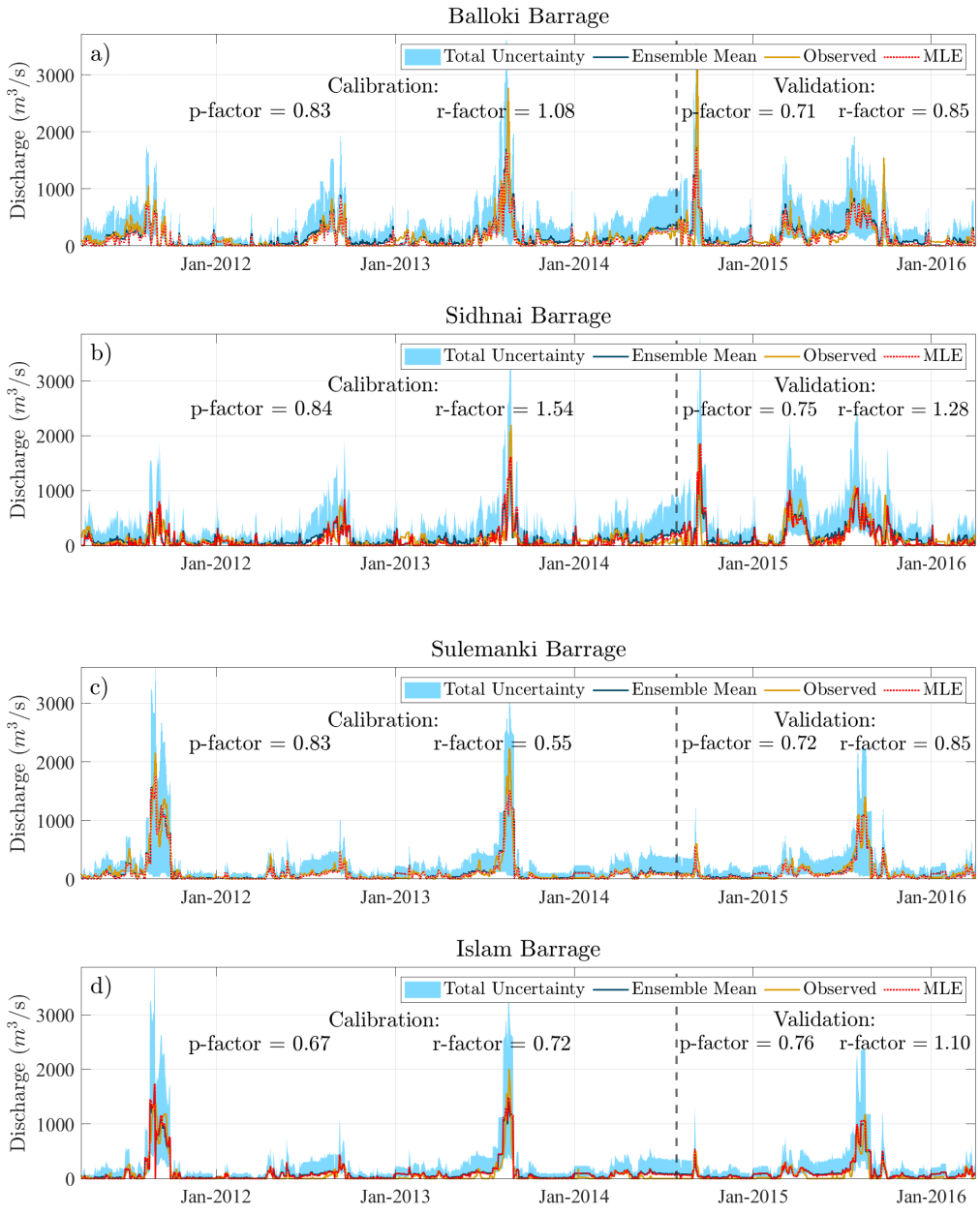

Figure 4.3.: Time series plot of Jhelum-Chenab zone with nodes lying on Ravi (a, b) and Sutlej (c, d) including Maximum Likelihood Estimate (MLE), Ensemble Mean, and observed values.

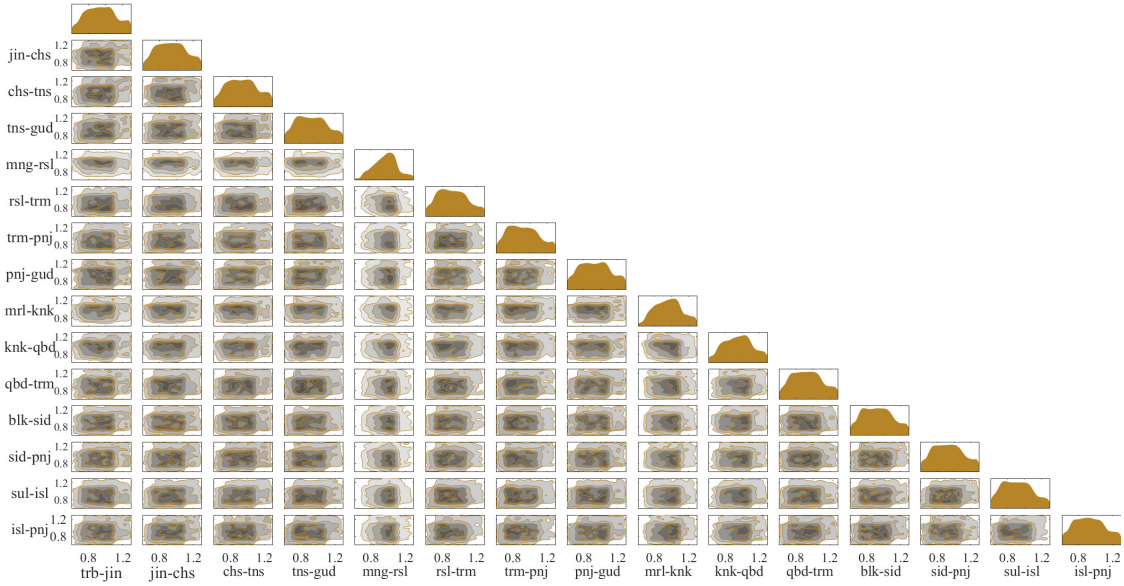

(a) Corner plot showing the results of the posterior river reaches.

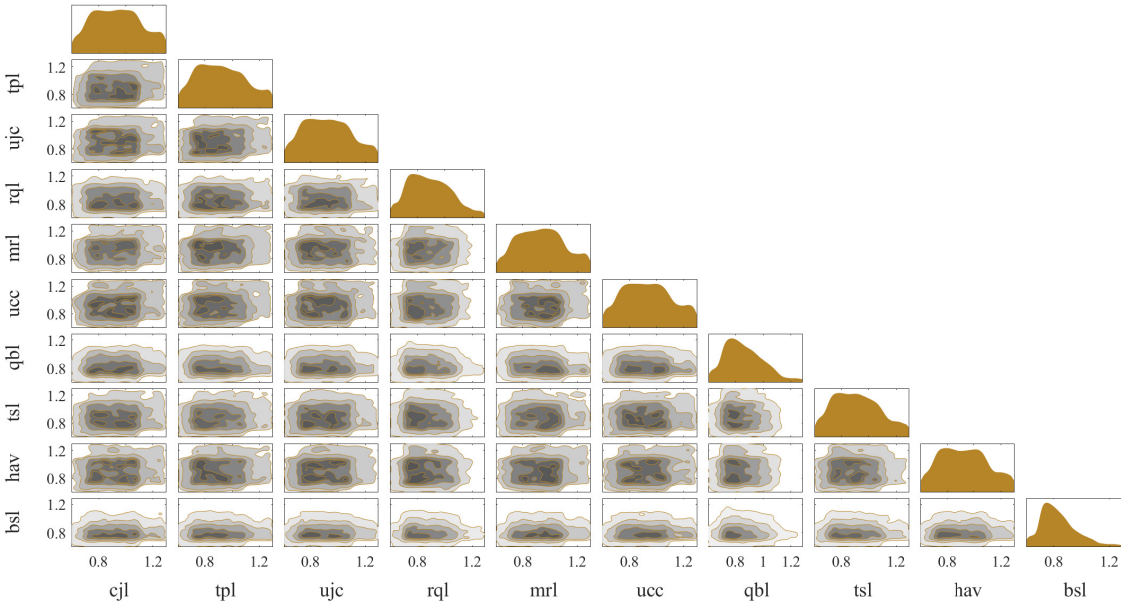

(b) Corner plot showing the results of the posterior link canals.

Figure 4.4.: Plot of posterior parameters. The distribution of each parameter is shown in the kernel smoothing density along the diagonal. The off-diagonal panel shows 2D joint posterior densities of each parameter, with contour levels of the joint probability densities at 10%, 20%, and 90% confidence intervals.

5. Discussions

Performance ratings for the recommended statistics at daily time step are presented in Table 4.1. According to the evaluation guidelines in [35], [28], and [29] for assessing the model performance, overall results in terms of NSE showed satisfactory values (>0.50). It is worth noting that the NSE value was high in Indus zone, oscillating between 0.76 and 0.94 during calibration and validation periods. On the other hand, in Jhelum-Chenab zone, the NSE indicates moderate, but still a satisfactory agreement between simulations and observations. This situation is in part because NSE measures the relative error; hence, small absolute errors can generate a large relative error at low discharges, resulting in low NSE values. Meanwhile, in Sidhnai barrage (Ravi river), NSE was below the threshold value. This larger discrepancy between observed and simulated discharges could be a result of the complex branching upstream of the barrage. Considering that the calibration was performed simultaneously for the entire system, and NSE>0.50 was achieved in 11 out of the 12 barrages, model performance in Sidhnai barrage is assumed to be satisfactory.

If the model performance is evaluated by using KGE indicator, the results show a good agreement between observations and simulations at most barrages, except for the validation period of Islam barrage (KGE=0.41). Albeit with high R^2 (0.75), this low KGE metric may occur because of variability, mean bias, and coefficient of variation of the observed discharges [24].

Accordingly, R^2 indicates that most of the observed dispersion is explained by the simulated discharge on all barrages. However, underestimation and overestimation are not accounted for by this index. By looking at the PBIAS evaluation guidelines, the distribution model can be judged as satisfactory ($+/-25\%$), suggesting a good representation of the overall water balance among the assessed sites. But, in some barrages, the simulations tend to be over− or even underestimated. For instance, calibration/validation at Chasma barrage indicated underestimation of simulated flows. Whereas, at Islam barrage, the PBIAS denoted a tendency of the network model to overestimate the simulations. From the above situation, differences in water balance between observed and simulated flow at Chasma and Islam are significantly high. This may explain the poor model performance in terms of KGE and NSE. At Punjnad barrage, PBIAS values also imply that the model overestimates simulated flow during calibration and underestimates it during validation.

In some cases like in Punjnad and Islam barrages, model performance was not similar in the validation period from that in the calibration period, as shown in Table 4.1. One probable reason would be that the hydroclimate conditions during the validation period

may change and do not behave as same as the hydrologic conditions in the calibration period [46].

To summarize, given the complexity of the irrigation system, with such a diversity of water uses and intense water management along the course of the rivers, the model behavior is considered satisfactory. However, there is a discrepancy between observed and simulated values at some nodes. Therefore, more local modeling with an improved algorithm would produce a better simulation. Of course, a calibration process is generally not sufficient to make well-informed decisions, as there is no guarantee that a model performs well under future climate conditions. In this context, uncertainty quantification associated with the hydrologic model is valuable.

Managing the Punjab Irrigation System requires an understanding of water losses and gains throughout the network. Losses include evaporation from barrages and infiltration from the river to groundwater. There are unmeasured water withdrawals within the network that is treated as losses, as well. On the other hand, gains include unmeasured contributions from minor tributaries and drains, direct runoffs, and exfiltration from groundwater. The obtained routing coefficients during the calibration process can explain the physical hydrologic dynamics in the region. For instance, in the Indus zone, net losses are high within the Jinnah-Chasma reach. These losses are partially compensated by moderate gains in the Tarbela-Jinnah and Chasma-Taunsa reaches. As suggested by previous studies, losses below Tarbela Dam are likely to be groundwater recharge which sustains the hot and dry parts of the basin. In the Jhelum-Chenab zone, there is a net gain overall (Mangla-Rasul, Marala-Qadirabad). Nevertheless, there are still significant net losses along the Rasul-Trimmu, Trimmu-Punjnad, and Qadirabad-Trimmu reaches. These losses are likely to be prime groundwater recharge for the lower agricultural areas. Such losses may partly be compensated by net gains in the Ravi river [1].

In general, model uncertainties are due to conceptual simplifications, processes taking place in the evaluated system but not included in the model, processes that are included in the model, but their occurrences are unaccountable because of limited data, and input quality data [43]. By analyzing the statistical indicators for quantifying uncertainties, the results showed that the Indus zone presents larger uncertainties as suggested by r-factor (average thickness of the uncertain band); nevertheless, there are quite larger observed data bracketed by the 2.5 and 97.5 percentile bands. It is known that a higher r-factor can be achieved only at the expense of a lower p-factor because both indicators are dependant on each other. Regarding the Jhelum-Chenab, Ravi, and Sutlej zone, overall results show small uncertainties, except at the Sidhnai barrage. These findings showed that zones with higher flow discharges are expected to be more sensitive to the uncertainties.

A major drawback in the Bayesian Monte Carlo sampling is that it may not converge toward the most probable region. This problem occurs when the parameters are non-informative and the prior range is too wide to incorporate all possible values. In this case, the probability of sampling the important region decreases. Conversely, if the prior range is kept small, there is a chance of cutting off important regions [47]. In

this manner, according to the posterior probability distribution shown in Figure 4.4, some of them may not efficiently determine the most probable value of the parameters accurately.

The decrease in measurement error (covariance matrix $\mathbf{R}$) affects the shape of the posterior distribution, as well as the weights of the likelihood function. By reducing measurement error (or increasing information in the data) the posterior uncertainty bands may shrink. However, given the complexity of the system and the extent of the evaluated area, this assumption may be incorrect.

Finally, by using the most complex models, calibration and uncertainty analysis methods may produce better results from what is shown here. However, a simple but robust model structure such as presented in this study can minimize the possibility of increasing the number of parameters and then reduce its uncertainty. Thus, the amount of parameter uncertainty quantified in this study may represent one of the optimistic cases from a hydrological modeling viewpoint.

6. Conclusions and Recommendations

In this study, a node-link network model was developed to characterize the irrigation system in Punjab province, Pakistan. The model was calibrated at the outflow of the barrages/headworks by using Bayesian Monte Carlo method. Particular attention was paid to quantifying the uncertainty of the output values.

Based on the results of this study, one can drawn the following conclusions:

- From the results, it has been demonstrated that satisfactory model performance can be achieved when using a simple model structure. Our results can be considered relatively robust given the complexity of the system and the extent of the evaluated area.
- The results in this study indicate a high model performance in the Indus zone; whereas, moderate model behavior in the Jhelum-Chenab zone.
- The lower NSE, PBIAS, and KGE values at Balloki, Sidhnai, and Sulemanki barrages suggest that the flexible modeling approach could take more training and setting up time, especially if it is used for predictions.
- The optimized routing coefficients reported by model calibration explained coherently the field conditions in the region. In this way, this modeling approach may help the water authorities to have an additional tool in decision-making processes to manage the irrigation system in the Punjab province.
- The posterior parameter distribution can shrink by reducing the measurement error. However, given the complexity of the system and the extent of the evaluated area, this assumption may be incorrect in this study.
- Findings in this study suggest that informative prior knowledge can help to reduce the uncertainty of model parameters and allow better assessment of the model outputs.
- Results in this study showed that zones with higher flow discharges are expected to be more sensitive to large uncertainties.

Some aspects have not been taken into account in this study, which can be seen as recommendations for future research.

- The proposed flexible hydrological model is an effective tool for understanding irrigation system dynamics in the Punjab province. Follow-up work to this study could focus on incorporating time lags as model parameters. It may lead to upgrading the model and help for approaching the issues of uncertainty due to model structures.

- Simulations in some barrage outflows (Balloki, Sidhnai, and Sulemanki) are relatively modest. Therefore, is recommended more local modeling with an improved algorithm.
- Despite the results of parameter calibration, the applicability of the model should be taken with great care because there are still uncertainties in the modeling results due to the conceptual nature and the quality of input data.
- This network model encompasses only up to the Tarbela Dam in Indus zone; therefore, the impact of reservoirs on the upstream of it needs to be analyzed.

A. Appendix

A.1. Main script file of network model framework created in MATLAB.

```
function sim = Distribution_model(mc_ujc, mc_mng_rsl, mc_rql,
    mc_rsl_trm, mc_ucc, mc_mrl, mc_mrl_knk,mc_knk_qbd, mc_qbl,
    mc_qbd_trm, mc_bsl, mc_blk_sid,mc_sul_isl, mc_isl_pnj,
    mc_trb_jin, mc_jin_chs, mc_cjl, mc_chs_tns, mc_tpl,
    mc_tns_gud, mc_tsl, mc_hav, mc_trm_pnj, mc_sid_pnj,
    mc_pnj_gud)
load('Distribution_data.mat') % for SI units
%% Mangla
dem.ass_ujc_int = zeros(length(dem.ujc_int), 1);
for i=1:length(dem.ujc_int)
    if dem.ujc_int(i) > coeff.cap_len(1)
        dem.ass_ujc_int(i)= coeff.cap_len(1);
    else
        dem.ass_ujc_int(i)= dem.ujc_int(i);
    end
end
dem.ass_ujc_l = zeros(length(dem.ujc_link), 1);
for i=1:length(dem.ujc_link)
    if dem.ujc_link(i) > coeff.cap_len(21)
        dem.ass_ujc_l(i)= coeff.cap_len(21);
    else
        dem.ass_ujc_l(i)= dem.ujc_link(i);
    end
end
av.av_ujc_link = inf.mng_out - dem.ass_ujc_int;
loss.loss_ujc_ht = round(dem.ass_ujc_l - dem.ass_ujc_l*mc_ujc);
inf.ujc_tail = dem.ass_ujc_l - loss.loss_ujc_ht;
% Arrival date
date.ujc_ard = date.initial + lag.lag_ujc;
date.ujc_adj = NaT(length(date.ujc_ard),1);
date.ujc_adj(1) = date.ujc_ard(2)-1;
for k = 2:length(date.initial)
```

```
    date.ujc_adj(k) = date.ujc_adj(k-1) +1;
29 end
   % Conversion from date to numbers
31 date.ujc_ard = datenum(date.ujc_ard);
   date.ujc_adj_numb = datenum(date.ujc_adj);
33 maxim.max_ujc = max(lag.lag_ujc);
   cont = 0;
35 % Time-lag adjustemnt
   for j = 1:length(date.initial)-maxim.max_ujc
37 cn =1;
   for i = 1: maxim.max_ujc
39 if date.ujc_adj_numb(j) == date.ujc_ard(j + i - 1)
   cont(cn) = inf.ujc_tail(j + i - 1);
41 end
   end
43 if isempty(cont) == 1
   cn = 1;
45 cont(cn) = inf.ujc_tail(j + i - 1);
   end
47 inf.ujc_adj_inf(j,1) = mean(cont);
   end
49 %% Alternative time_lag adjustment
   adj_t.ujc_unique = unique(date.ujc_adj_numb(:,1));
51 adj_t.ujc = accumarray(date.ujc_ard,inf.ujc_tail, [],@mean);
   inf.ujc_adj_inf = adj_t.ujc(adj_t.ujc_unique);
53 %%
   % Maximum capacity of canals and links
55 inf.dsrel_mng = zeros(length(inf.mng_out), 1);
   for i=1:length(inf.mng_out)
57 if inf.mng_out(i) - dem.ass_ujc_int(i) - dem.ass_ujc_l(i) < 0
       inf.dsrel_mng(i) = 0;
59 else
       inf.dsrel_mng(i) = inf.mng_out(i) - dem.ass_ujc_int(i) -
          dem.ass_ujc_l(i);
61 end
   end
63 .
   .
65 .
   % Similar code structure is applied for remaining barrages
67 end
```

Link-network model of Punjab Irrigation System.

A.2. Volume difference between observed and simulated model for Kharif and Rabi season.

Pakistan has two crop seasons named "Kharif" and "Rabi". Kharif refers to the summer growing period (beginning of the first rains) starting from April to the end of September, with major crops being rice, corn and cotton. Rabi or dry sowing season, begins in October and is harvested at the end of March. The main Rabi crops include wheat, barley, and millet.

Table A.1.: Volume difference (ΔV) between observed and simulated results in Indus and Jhelum-Chenab zones.

Year	**Jinnah** $\mathbf{m^3}$	**Chasma** $\mathbf{m^3}$	**Taunsa** $\mathbf{m^3}$	**Rasul** $\mathbf{m^3}$	**Khanki** $\mathbf{m^3}$	**Qadirabad** $\mathbf{m^3}$
2011-I	-72323	183515	108228	-2692	22553	-11388
2011-II	-26448	22325	18975	8409	2825	-1840
2012-I	-52054	214389	104285	-7614	14	-15908
2012-II	-13017	58910	45907	5102	-7654	-6652
2013-I	-86435	308628	140047	249	2173	-20992
2013-II	8763	50494	41223	8752	-1672	-1539
2014-I	-61079	202561	134371	-161	-1119	-24782
2014-II	14060	73750	54925	-27703	6593	2520
2015-I	-72374	325745	207072	-26222	-727	-19883
2015-II	31256	77814	56344	-19344	1192	4700

Table A.2.: Volume difference (ΔV) between observed and simulated results in Ravi and Sutlej zones.

Year	**Trimmu** $\mathbf{m^3}$	**Balloki** $\mathbf{m^3}$	**Sidhnai** $\mathbf{m^3}$	**Sulemanki** $\mathbf{m^3}$	**Islam** $\mathbf{m^3}$	**Punjnad** $\mathbf{m^3}$
2011-I	13144	15838	7707	10887	-158	-22029
2011-II	1391	896	1394	1858	-247	-6381
2012-I	-5352	1388	-2755	4087	-6765	-27567
2012-II	1772	5145	5340	-1230	-4534	-1140
2013-I	9205	3191	-4075	1241	-10013	-20526
2013-II	6859	6360	5068	-641	-4160	6734
2014-I	24365	1694	-16248	1598	-8040	-11990
2014-II	20215	1771	4396	-2050	-3388	26240
2015-I	25498	1981	5638	4167	-14028	-78
2015-II	17175	822	755	850	-5185	19045

A.3. Simulated and observed volumes for Kharif and Rabi.

Table A.3.: Barrage downstream volumes of observed and simulated values during Kharif season (April to September).

Barrage	**Volume (m^3)**	**2011-I**	**2012-I**	**2013-I**	**2014-I**	**2015-I**
Jinnah	Obs	750334	748770	921037	753947	974763
	Sim	822657	800824	1007472	815026	1047137
Percent bias	%	9.6	7.0	9.4	8.1	7.4
Chasma	Obs	754113	770175	1001843	782274	1082466
	Sim	570598	555786	693215	579713	756721
Percent bias	%	-24.3	-27.8	-30.8	-25.9	-30.1
Taunsa	Obs	626198	623585	781178	655223	933027
	Sim	517970	519300	641131	520852	725955
Percent bias	%	-17.3	-16.7	-17.9	-20.5	-22.2
Rasul	Obs	69715	61301	45596	114115	123425
	Sim	72407	68915	45347	114276	149647
Percent bias	%	3.9	12.4	-0.5	0.1	21.2
Trimmu	Obs	99676	64109	119489	168839	229087
	Sim	86532	69461	110284	144474	203589
Percent bias	%	-13.2	8.3	-7.7	-14.4	-11.1
Punjnad	Obs	76635	35578	119330	116535	213750
	Sim	98664	63145	139856	128525	213828
Percent bias	%	28.7	77.5	17.2	10.3	0.04
Khanki	Obs	144003	131615	168842	190118	194321
	Sim	121450	131601	166669	191237	195048
Percent bias	%	-15.7	0.0	-1.3	0.6	0.4
Qadirabad	Obs	88801	71530	119909	139073	166880
	Sim	100189	87438	140901	163855	186763
Percent bias	%	12.8	22.2	17.5	17.8	11.9
Balloki	Obs	41776	25064	46017	45960	53719
	Sim	25938	23676	42826	44266	51738
Percent bias	%	-37.9	-5.5	-6.9	-3.7	-3.7
Sidhnai	Obs	24454	15234	27752	20220	55067
	Sim	16747	17989	31827	36468	49429
Percent bias	%	-31.5	18.1	14.7	80.4	-10.2
Sulemanki	Obs	65789	18665	42211	16219	47152
	Sim	54902	14578	40970	14621	42985
Percent bias	%	-16.5	-21.9	-2.9	-9.9	-8.8
Islam	Obs	46775	7532	30275	6326	28211
	Sim	46933	14297	40288	14366	42239
Percent bias	%	0.3	89.8	33.1	127.1	49.7

Table A.4.: Barrage downstream volumes of observed and simulated values during Rabi season (October to March).

Barrage	**Volume (m^3)**	**2011-II**	**2012-II**	**2013-II**	**2014-II**	**2015-II**
Jinnah	Obs	226421	267880	264139	255793	244966
	Sim	252869	280897	255376	241733	213710
Percent bias	%	11.7	4.9	-3.3	-5.5	-12.8
Chasma	Obs	192089	247655	234392	242029	229828
	Sim	169764	188745	183898	168279	152014
Percent bias	%	-11.6	-23.8	-21.5	-30.5	-33.9
Taunsa	Obs	172264	214625	209461	206650	193732
	Sim	153289	168718	168238	151725	137388
Percent bias	%	-11.0	-21.4	-19.7	-26.6	-29.1
Rasul	Obs	43789	43527	58791	84473	96313
	Sim	35380	38425	50039	112176	115657
Percent bias	%	-19.2	-11.7	-14.9	32.8	20.1
Trimmu	Obs	13122	19521	23977	84035	73356
	Sim	11731	17749	17118	63820	56181
Percent bias	%	-10.6	-9.1	-28.6	-24.1	-23.4
Punjnad	Obs	12384	14809	18741	75628	62981
	Sim	18765	15949	12007	49388	43936
Percent bias	%	51.5	7.7	-35.9	-34.7	-30.2
Khanki	Obs	9273	23533	22289	44107	24266
	Sim	6448	31187	23961	37514	23074
Percent bias	%	-30.5	32.5	7.5	-14.9	-4.9
Qadirabad	Obs	6500	14086	14648	34401	26571
	Sim	8340	20738	16187	31881	21871
Percent bias	%	28.3	47.2	10.5	-7.3	-17.7
Balloki	Obs	4377	9770	13602	15141	6720
	Sim	3481	4625	7242	13370	5898
Percent bias	%	-20.5	-52.7	-46.8	-11.7	-12.2
Sidhnai	Obs	7958	8762	9968	20258	10384
	Sim	6564	3422	4900	15862	9629
Percent bias	%	-17.5	-60.9	-50.8	-21.7	-7.3
Sulemanki	Obs	3807	5567	5853	7590	10461
	Sim	1949	6797	6494	9640	9611
Percent bias	%	-48.8	22.1	11.0	27.0	-8.1
Islam	Obs	1681	2136	2192	6087	4232
	Sim	1928	6670	6352	9475	9417
Percent bias	%	14.7	212.3	189.8	55.7	122.5

A.4. Model performance and posterior parameters.

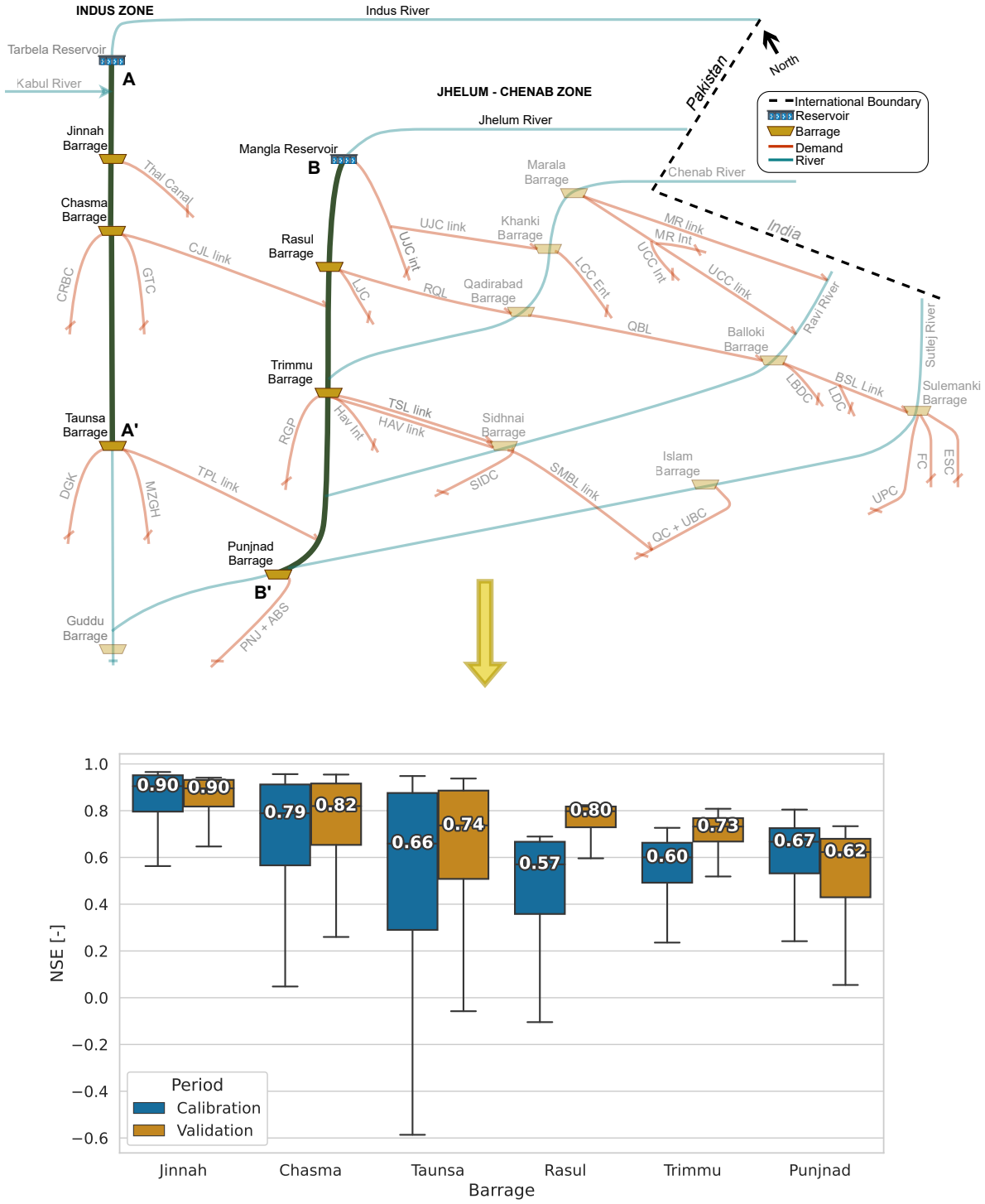

Figure A.1.: Results of model performance for the section A-A' and B-B' in network model. The values in the boxplot depict the median of NSE for calibration and validation periods.

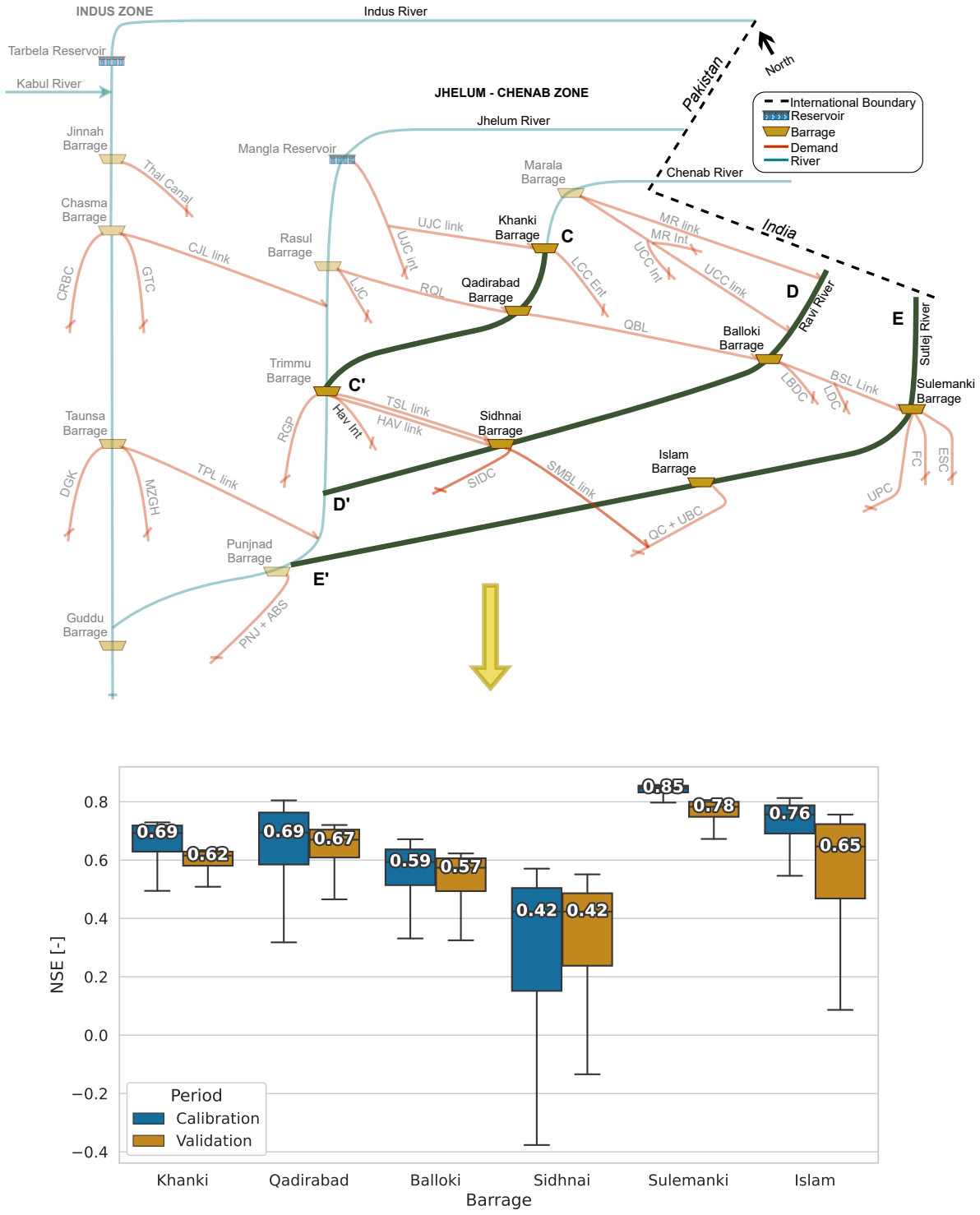

Figure A.2.: Results of model performance for the section C-C', D-D' and E-E' in network model. The values in the boxplot depict the median of NSE for calibration and validation periods.

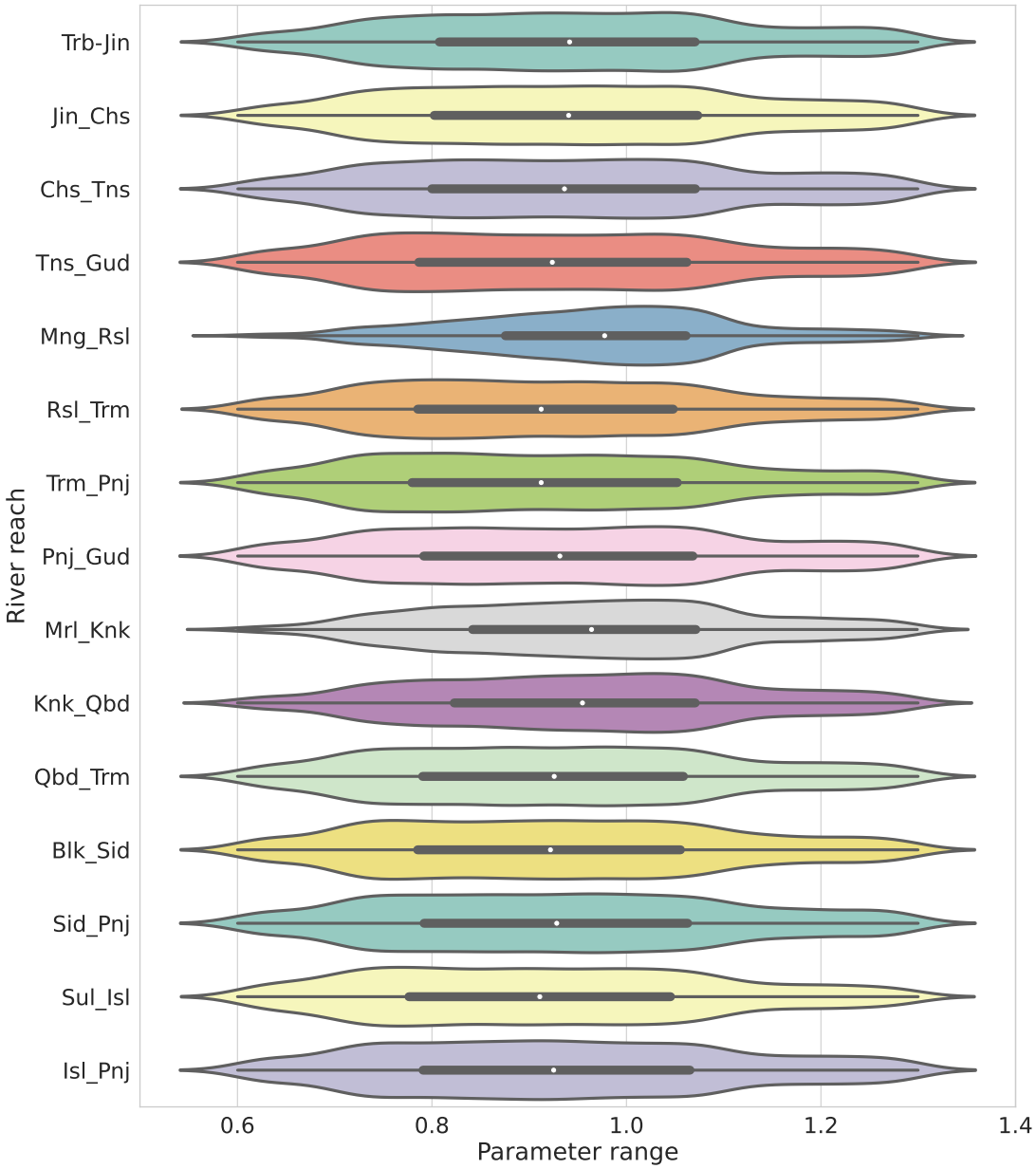

Figure A.3.: Violin plot of posterior river reach parameters, representing a combination of the box plot with a kernel density plot.

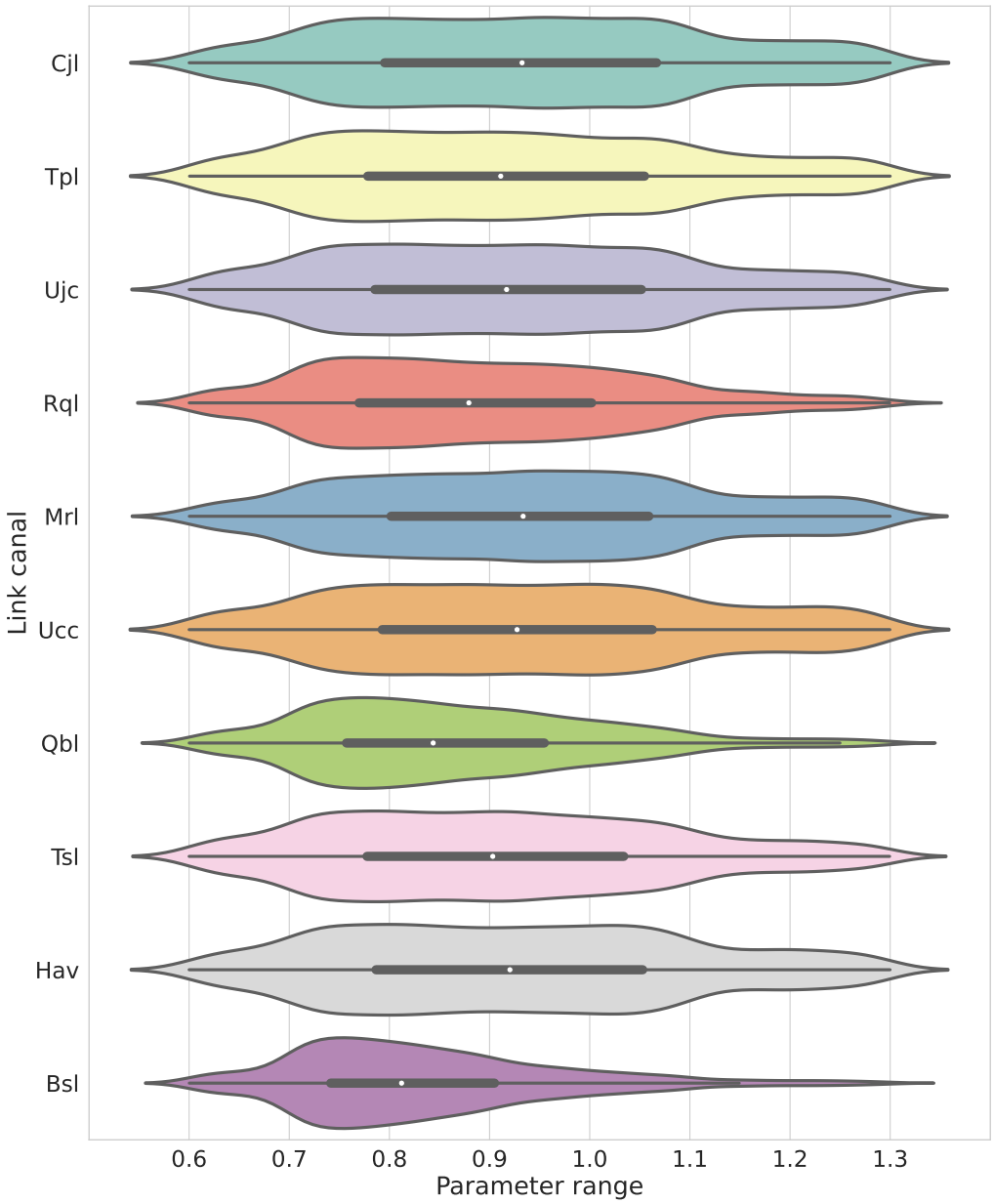

Figure A.4.: Violin plot of posterior link canal parameters. The white dot represents the median and the thick gray bar in the center represents the interquartile range.

Bibliography

[1] William J Young, Arif Anwar, Tousif Bhatti, Edoardo Borgomeo, Stephen Davies, William R Garthwaite III, E Michael Gilmont, Christina Leb, Lucy Lytton, Ian Makin, et al. *Pakistan: Getting more from water*. World Bank, 2019.

[2] Peter H Gleick. *The world's water 1998-1999: the biennial report on freshwater resources*. Island Press, 1998.

[3] Peter Kreins, Martin Henseler, Jano Anter, Frank Herrmann, and Frank Wendland. Quantification of climate change impact on regional agricultural irrigation and groundwater demand. *Water resources management*, 29(10):3585–3600, 2015.

[4] Julien Lerat, Chas Egan, Shaun Kim, Matt Gooda, Alex Loy, Quanxi Shao, and Cuan Petheram. Calibration of river models for the flinders and gilbert catchments. In *A Technical Report to the Australian Government From the CSIRO Flinders and Gilbert Agricultural Resource Assessment, Part of the North Queensland Irrigated Agriculture Strategy*. CSIRO Water for a Healthy Country and Sustainable Agriculture flagships, 2013.

[5] Xue Wen Wu, Ling Li, and Yong Gang Qu. Modelling and analysis of river networks based on complex networks theory. In *Advanced Materials Research*, volume 756, pages 2728–2733. Trans Tech Publ, 2013.

[6] David Rassam, Ian Jolly, and Trevor Pickett. Guidelines for modelling groundwater-surface water interactions in ewater source: Towards best practice model application. 2012.

[7] John K Kruschke and Torrin M Liddell. Bayesian data analysis for newcomers. *Psychonomic bulletin & review*, 25(1):155–177, 2018.

[8] Rens van de Schoot, Sarah Depaoli, Ruth King, Bianca Kramer, Kaspar Märtens, Mahlet G Tadesse, Marina Vannucci, Andrew Gelman, Duco Veen, Joukje Willemsen, et al. Bayesian statistics and modelling. *Nature Reviews Methods Primers*, 1(1):1–26, 2021.

[9] Yeojin Chung, Andrew Gelman, Sophia Rabe-Hesketh, Jingchen Liu, and Vincent Dorie. Weakly informative prior for point estimation of covariance matrices in hierarchical models. *Journal of Educational and Behavioral Statistics*, 40(2):136–157, 2015.

[10] Huarui Zhang. *Monte Carlo Methods in Bayesian Inference: Theory, Methods and Applications*. University of Arkansas, 2016.

[11] Anneli Schöniger. *Bayesian assessment of conceptual uncertainty in hydrosystem modeling*. PhD thesis, Universitätsbibliothek Tübingen, 2016.

[12] Daniela Balin Talamba, Eric Parent, and André Musy. Bayesian multiresponse calibration of TOPMODEL: Application to the haute-mentue catchment, Switzerland. *Water Resources Research*, 46(8), 2010.

[13] William M Bolstad and James M Curran. *Introduction to Bayesian statistics*. John Wiley & Sons, 2016.

[14] Viviane Borda Pinheiro, Mauro Naghettini, and Luiz Rafael Palmier. Uncertainty estimation in hydrodynamic modeling using bayesian techniques. *RBRH*, 24, 2019.

[15] Soroosh Sorooshian and John A Dracup. Stochastic parameter estimation procedures for hydrologie rainfall-runoff models: Correlated and heteroscedastic error cases. *Water Resources Research*, 16(2):430–442, 1980.

[16] Zhaoyuan Li and Jianfeng Yao. Testing for heteroscedasticity in high-dimensional regressions. *Econometrics and statistics*, 9:122–139, 2019.

[17] Mark Thyer, Benjamin Renard, Dmitri Kavetski, George Kuczera, Stewart William Franks, and Sri Srikanthan. Critical evaluation of parameter consistency and predictive uncertainty in hydrological modeling: A case study using bayesian total error analysis. *Water Resources Research*, 45(12), 2009.

[18] Gerrit Schoups and Jasper A Vrugt. A formal likelihood function for parameter and predictive inference of hydrologic models with correlated, heteroscedastic, and non-gaussian errors. *Water Resources Research*, 46(10), 2010.

[19] Robert L Kaufman. *Heteroskedasticity in regression: Detection and correction*. Sage Publications, 2013.

[20] George EP Box and David R Cox. An analysis of transformations. *Journal of the Royal Statistical Society: Series B (Methodological)*, 26(2):211–243, 1964.

[21] David R Legates and Gregory J McCabe Jr. Evaluating the use of "goodness-of-fit" measures in hydrologic and hydroclimatic model validation. *Water resources research*, 35(1):233–241, 1999.

[22] Xiaohui Zhong and Utpal Dutta. Engaging nash-sutcliffe efficiency and model efficiency factor indicators in selecting and validating effective light rail system operation and maintenance cost models. *Journal of Traffic and Transportation Engineering*, 3:255–265, 2015.

[23] Peter Krause, DP Boyle, and Frank Bäse. Comparison of different efficiency criteria for hydrological model assessment. *Advances in geosciences*, 5:89–97, 2005.

[24] Wouter JM Knoben, Jim E Freer, and Ross A Woods. Inherent benchmark or not? comparing nash–sutcliffe and kling–gupta efficiency scores. *Hydrology and Earth System Sciences*, 23(10):4323–4331, 2019.

[25] Hoshin Vijai Gupta and Harald Kling. On typical range, sensitivity, and normalization of mean squared error and nash-sutcliffe efficiency type metrics. *Water Resources Research*, 47(10), 2011.

[26] Chesheng Zhan, Jian Han, Lei Zou, Fubao Sun, and Tiejun Wang. Heteroscedastic and symmetric efficiency for hydrological model evaluation criteria. *Hydrology Research*, 50(5):1189–1201, 2019.

[27] Hugo Henrique Cardoso de Salis, Adriana Monteiro da Costa, Joao Herbert Moreira Vianna, Marysol Azeneth Schuler, Annika Künne, Luis Filipe Sanches Fernandes, and Fernando Antonio Leal Pacheco. Hydrologic modeling for sustainable water resources management in urbanized karst areas. *International journal of environmental research and public health*, 16(14):2542, 2019.

[28] Daniel N Moriasi, Jeffrey G Arnold, Michael W Van Liew, Ronald L Bingner, R Daren Harmel, and Tamie L Veith. Model evaluation guidelines for systematic quantification of accuracy in watershed simulations. *Transactions of the ASABE*, 50(3):885–900, 2007.

[29] Daniel N Moriasi, Margaret W Gitau, Naresh Pai, and Prasad Daggupati. Hydrologic and water quality models: Performance measures and evaluation criteria. *Transactions of the ASABE*, 58(6):1763–1785, 2015.

[30] Axel Ritter and Rafael Munoz-Carpena. Performance evaluation of hydrological models: Statistical significance for reducing subjectivity in goodness-of-fit assessments. *Journal of Hydrology*, 480:33–45, 2013.

[31] Raji Pushpalatha, Charles Perrin, Nicolas Le Moine, and Vazken Andréassian. A review of efficiency criteria suitable for evaluating low-flow simulations. *Journal of Hydrology*, 420:171–182, 2012.

[32] Hoshin V Gupta, Harald Kling, Koray K Yilmaz, and Guillermo F Martinez. Decomposition of the mean squared error and nse performance criteria: Implications for improving hydrological modelling. *Journal of hydrology*, 377(1-2):80–91, 2009.

[33] Sandra Pool, Marc Vis, and Jan Seibert. Evaluating model performance: towards a non-parametric variant of the kling-gupta efficiency. *Hydrological Sciences Journal*, 63(13-14):1941–1953, 2018.

[34] Hoshin Vijai Gupta, Soroosh Sorooshian, and Patrice Ogou Yapo. Status of automatic calibration for hydrologic models: Comparison with multilevel expert calibration. *Journal of hydrologic engineering*, 4(2):135–143, 1999.

[35] KC Abbaspour. Swat calibration and uncertainty programs: A user manual. *Swiss Federal Institute of Aquatic Science and Technology: Eawag, Switzerland*, 2015.

[36] Muhammad Abid, Jürgen Scheffran, Uwe A Schneider, and MJESD Ashfaq. Farmers' perceptions of and adaptation strategies to climate change and their determinants: the case of Punjab province, Pakistan. *Earth System Dynamics*, 6(1):225–243, 2015.

[37] Ghulam Hussain Dars, Bakhshal Khan Lashari, Mehran Sattar Soomro, Courtenay Strong, and Kamran Ansari. Pakistan's water resources in the era of climate change. *Water Resources of Pakistan: Issues and Impacts*, 9:95, 2021.

[38] Waqas Ahmed, Muhammad Naseer Rais, Rakhshanda Bano, Kazi Tamaddun, and Sajjad Ahmad. Water sharing, governance, and management among the provinces in Pakistan using evidence-based decision support system. In *World Environmental and Water Resources Congress 2018: Watershed Management, Irrigation and Drainage, and Water Resources Planning and Management*, pages 220–233. American Society of Civil Engineers Reston, VA, 2018.

[39] Muhammad Abid, Mohsin Hafeez, and Muhammad Arif Watto. Sustainability analysis of Irrigation Water Management in Punjab, Pakistan. *Water Resources of Pakistan: Issues and Impacts*, 9:133, 2021.

[40] Sergey Oladyshkin, Holger Class, and Wolfgang Nowak. Bayesian updating via bootstrap filtering combined with data-driven polynomial chaos expansions: methodology and application to history matching for carbon dioxide storage in geological formations. *Computational Geosciences*, 17(4):671–687, 2013.

[41] Ana Clara Lazzari Franco and Nadia Bernardi Bonumá. Multi-variable SWAT model calibration with remotely sensed evapotranspiration and observed flow. *RBRH*, 22, 2017.

[42] Abolanle E Odusanya, Bano Mehdi, Christoph Schürz, Adebayo O Oke, Olufiropo S Awokola, Julius A Awomeso, Joseph O Adejuwon, and Karsten Schulz. Multi-site calibration and validation of SWAT with satellite-based evapotranspiration in a data-sparse catchment in southwestern nigeria. *Hydrology and Earth System Sciences*, 23(2):1113–1144, 2019.

[43] Karim C Abbaspour, Elham Rouholahnejad, SRINIVASANB Vaghefi, Raghavan Srinivasan, Hong Yang, and Bjørn Kløve. A continental-scale hydrology and water quality model for europe: Calibration and uncertainty of a high-resolution large-scale SWAT model. *Journal of hydrology*, 524:733–752, 2015.

[44] Boini Narsimlu, Ashvin K Gosain, Baghu R Chahar, Sudhir Kumar Singh, and Prashant K Srivastava. SWAT model calibration and uncertainty analysis for streamflow prediction in the Kunwari River Basin, India, using sequential uncertainty fitting. *Environmental Processes*, 2(1):79–95, 2015.

[45] Jing Yang, Peter Reichert, Karim C Abbaspour, Jun Xia, and Hong Yang. Comparing uncertainty analysis techniques for a SWAT application to the Chaohe Basin in China. *Journal of hydrology*, 358(1-2):1–23, 2008.

[46] Yuqiong Liu and Hoshin V Gupta. Uncertainty in hydrologic modeling: Toward an integrated data assimilation framework. *Water resources research*, 43(7), 2007.

[47] Song S Qian, Craig A Stow, and Mark E Borsuk. On monte carlo methods for bayesian inference. *Ecological modelling*, 159(2-3):269–277, 2003.